

August 2013

Thesis for Master Degree

**Coumarins as porcine epidemic diarrhea  
virus (PEDV) inhibitors from  
*Saposhnikovia divaricata***

Chosun University Graduate School

Department of Pharmacy

Sharma Govinda

**Coumarins as porcine epidemic diarrhea  
virus (PEDV) inhibitors from  
*Saposhnikovia divaricata***

방풍으로부터 PEDV 바이러스 저해물질로서 코마린 화합물의  
분리 및 활성 규명

2013 년 08 월 23 일

Chosun University Graduate School  
Department of Pharmacy  
Sharma Govinda

**Coumarins as porcine epidemic diarrhea  
virus (PEDV) inhibitors from  
*Saposhnikovia divaricata***

지도교수 최홍석

공동 지도 교수 오 원 근

이 논문을 약학 석사학위신청 논문으로 제출함

2013 년 04 월

조선대학교 대학원

약학과

샤르마 고빈다

This thesis is examined and approved for  
Sharma Govinda's master degree

Chairman Chosun Univ.

Prof. Choi Hoo Kyun (인)



Member Seoul National Univ.

Prof. Kang Keon Wook (인)



Member Chosun Univ.

Prof. Choi Hong Seok (인)



2013년 05월

Chosun University Graduate School

# Contents

<b>Contents.....</b>	<b>i</b>
<b>List of schemes.....</b>	<b>iv</b>
<b>List of tables.....</b>	<b>v</b>
<b>List of figures.....</b>	<b>vi</b>
<b>List of abbreviations.....</b>	<b>viii</b>
<b>Abstract.....</b>	<b>x</b>
<b>1. Introduction.....</b>	<b>1</b>
1.1. Porcine epidemic diarrhea (PED).....	1
1.2. The virus.....	2
1.2.1. Coronavirus.....	3
1.2.2. Evolution.....	6
1.2.3. Porcine epidemic diarrhea virus (PEDV).....	7
1.3. Vaccines.....	7
1.4. <i>Saposhnikovia divaricata</i> (Apiaceae).....	8
<b>2. Material and Methods.....</b>	<b>12</b>
2.1. Materials.....	12
2.1.1. Plant material.....	12
2.1.2. Chemicals, reagents and chromatography.....	12
2.2. Methods.....	13
2.2.1. Extraction and isolation.....	13
2.2.2. Viruses and cell.....	16
2.2.3. Cytopathic effect (CPE) inhibition.....	16

2.2.3.1. Cytopathic effect.....	16
2.2.3.2. CPE inhibition assay.....	17
2.2.3.3. TCID <sub>50</sub> (50 % Tissue culture infectious dose).....	18
2.2.4. MTT assay.....	18
2.2.5. Statistical analysis.....	19
<b>3. Results and Discussions.....</b>	<b>20</b>
3.1. Isolation of compounds from radix of <i>S. divaricata</i> .....	20
3.2. Structures of isolated compounds.....	20
3.3. Structure determination of isolated compounds.....	21
3.3.1. Structure determination of compound <b>1</b> .....	21
3.3.2. Structure determination of compound <b>2</b> .....	27
3.3.3. Structure determination of compound <b>3</b> .....	29
3.3.4. Structure determination of compound <b>4</b> .....	31
3.3.5. Structure determination of compound <b>5</b> .....	33
3.3.6. Structure determination of compound <b>6</b> .....	35
3.3.7. Structure determination of compound <b>7</b> .....	36
3.3.8. Structure determination of compound <b>8</b> .....	37
3.3.9. Structure determination of compound <b>9</b> .....	39
3.3.10. Structure determination of compound <b>10</b> .....	40
3.4. Effect of isolated compounds on PED virus induced CPE.....	42
3.4.1. Determination of TCID <sub>50</sub> of stock PED virus suspension.....	42
3.4.2. Assessment of PEDV induced CPE inhibitory activities of isolated compounds	43
<b>4. Conclusions.....</b>	<b>48</b>

<b>5. References.....</b>	<b>49</b>
<b>6. Acknowledgements.....</b>	<b>58</b>

## List of Schemes

<b>Scheme 1.</b> Isolation scheme of compounds from radix of <i>S. divaricata</i> .....	15
---	----



## List of Tables

<b>Table 1.</b> Classification of Coronavirus.....	5
<b>Table 2.</b> $^1\text{H}$ and $^{13}\text{C}$ NMR of compound <b>1</b> , <b>2</b> and <b>3</b> .....	30
<b>Table 3.</b> $^1\text{H}$ and $^{13}\text{C}$ NMR of compound <b>4</b> , <b>5</b> and <b>6</b> .....	35
<b>Table 4.</b> $^1\text{H}$ and $^{13}\text{C}$ NMR of compound <b>7</b> and <b>8</b> .....	38
<b>Table 5.</b> $^1\text{H}$ and $^{13}\text{C}$ NMR of compound <b>9</b> and <b>10</b> .....	41
<b>Table 6.</b> Inhibitory effects of compounds <b>1</b> to <b>10</b> on PEDV induced CPE.....	44

## List of figures

<b>Figure 1.</b> Microscope photograph and schematic diagram of Coronavirus.....	3
<b>Figure 2.</b> Replication machinery of Coronavirus.....	4
<b>Figure 3.</b> Evolution of Coronaviruses.....	6
<b>Figure 4.</b> <i>Saposhnikovia divaricata</i> — 1. Root with branch; 2. Branch with flowers; 3. Sliced dry herb.....	11
<b>Figure 5.</b> Structure of compounds ( <b>1</b> to <b>10</b> ) isolated from radix of <i>S. divaricata</i> .....	20
<b>Figure 6.</b> <sup>1</sup> H-NMR spectrum of compound <b>1</b> (500 MHz, CDCl <sub>3</sub> ).....	21
<b>Figure 7.</b> <sup>13</sup> C-NMR spectrum of compound <b>1</b> (125 MHz, CDCl <sub>3</sub> ).....	22
<b>Figure 8.</b> HMBC spectrum of Compound <b>1</b> .....	23
<b>Figure 9.</b> HSQC spectrum of compound <b>1</b> .....	24
<b>Figure 10.</b> Key HMBC [H (solid arrow) C] Correlations for compound <b>1</b> .....	25
<b>Figure 11.</b> Low resolution EI-Mass Spectrum for compound <b>1</b> .....	26
<b>Figure 12.</b> <sup>1</sup> H-NMR spectrum of compound <b>2</b> (300 MHz, acetone- <i>d</i> <sub>6</sub> ).....	27
<b>Figure 13.</b> <sup>13</sup> C-NMR spectrum of compound <b>2</b> (75 MHz, acetone- <i>d</i> <sub>6</sub> ).....	28
<b>Figure 14.</b> <sup>1</sup> H-NMR spectrum of compound <b>3</b> (300 MHz, acetone- <i>d</i> <sub>6</sub> ).....	29
<b>Figure 15.</b> <sup>13</sup> C-NMR spectrum of compound <b>3</b> (75 MHz, acetone- <i>d</i> <sub>6</sub> ).....	29
<b>Figure 16.</b> <sup>1</sup> H-NMR spectrum of compound <b>4</b> (300 MHz, acetone- <i>d</i> <sub>6</sub> ).....	31
<b>Figure 17.</b> <sup>13</sup> C-NMR spectrum of compound <b>4</b> (75 MHz, acetone- <i>d</i> <sub>6</sub> ).....	31
<b>Figure 18.</b> <sup>1</sup> H-NMR spectrum of compound <b>5</b> (300 MHz, acetone- <i>d</i> <sub>6</sub> ).....	32
<b>Figure 19.</b> <sup>13</sup> C-NMR spectrum of compound <b>5</b> (75 MHz, acetone- <i>d</i> <sub>6</sub> ).....	33
<b>Figure 20.</b> <sup>1</sup> H-NMR spectrum of compound <b>6</b> (500 MHz, acetone- <i>d</i> <sub>6</sub> ).....	34
<b>Figure 21.</b> <sup>13</sup> C-NMR spectrum of compound <b>6</b> (125 MHz, acetone- <i>d</i> <sub>6</sub> ).....	34

<b>Figure 22.</b> <sup>1</sup> H-NMR spectrum of compound <b>7</b> (300 MHz, acetone- <i>d</i> <sub>6</sub> ).....	36
<b>Figure 23.</b> <sup>13</sup> C-NMR spectrum of compound <b>7</b> (75 MHz, acetone- <i>d</i> <sub>6</sub> ).....	36
<b>Figure 24.</b> <sup>1</sup> H-NMR spectrum of compound <b>8</b> (500 MHz, acetone- <i>d</i> <sub>6</sub> ).....	37
<b>Figure 25.</b> <sup>13</sup> C-NMR spectrum of compound <b>8</b> (125 MHz, acetone- <i>d</i> <sub>6</sub> ).....	37
<b>Figure 26.</b> <sup>1</sup> H-NMR spectrum of compound <b>9</b> (300 MHz, acetone- <i>d</i> <sub>6</sub> ).....	39
<b>Figure 27.</b> <sup>13</sup> C-NMR spectrum of compound <b>9</b> (75 MHz, acetone- <i>d</i> <sub>6</sub> ).....	39
<b>Figure 28.</b> <sup>1</sup> H-NMR spectrum of compound <b>10</b> (300 MHz, acetone- <i>d</i> <sub>6</sub> ).....	40
<b>Figure 29.</b> <sup>13</sup> C-NMR spectrum of compound <b>10</b> (75 MHz, acetone- <i>d</i> <sub>6</sub> ).....	41
<b>Figure 30.</b> PED virus titration curve for TCID <sub>50</sub> determination.....	42
<b>Figure 31.</b> A. Khellactone (angular pyrano coumarin) skeleton; B. Compound <b>1</b> ; C. Compound <b>2</b> ; D. Compound <b>6</b> .....	43
<b>Figure 32.</b> CPE inhibitory activity (black dots) and cell survival data (white dots) of compound <b>2</b> (A) and <b>6</b> (B).....	45
<b>Figure 33.</b> Dose dependent activity of Compound <b>1</b> (A), <b>3</b> (B), <b>4</b> (C) and <b>5</b> (D) against PEDV induced CPE in vero cells.....	46
<b>Figure 34.</b> Morphologies of vero cells show the effects of compound <b>1</b> , <b>2</b> and compounds used as positive controls, rivabirin and glycirrhizin on PEDV-induced CPE.....	47

## List of Abbreviations

ATPase	Adenosine triphosphatase
BCoV	Bovine coronavirus
CCoV	Canine coronavirus
CoV	Coronavirus
EIMS	Electron impact mass spectrometry
EtOAc	Ethyl acetate
FCoV	Feline coronavirus
HCoV	Human coronavirus
HPLC	High performance liquid chromatography
IBV	Infectious bronchitis virus
MeOH	Methanol
MHV	Mouse hepatitis virus
MTT	(3-(4,5-Dimethylthiazol-2-yl)-2,5-diphenyltetrazolium bromide
ORF	Open reading frame
PED	Porcine epidemic diarrhea
PEDV	Porcine epidemic diarrhea virus
PRRS	Porcine reproductive and respiratory syndrome
PRRSV	Porcine reproductive and respiratory syndrome virus
RNA	Ribonucleic acid
SARS-CoV	Severe acute respiratory syndrome – Coronavirus
SD	Standard deviation
TCM	Traditional Chinese medicine

TGE	Transmissible gastroenteritis
TGEV	Transmissible gastroenteritis virus
TLC	Thin layer chromatography
TMS	Tetra methyl silane

## (국문 초록)

# 방풍으로부터 PEDV 바이러스 저해물질로서 코마린 화합물의 분리 및 활성 규명

샤르마 고빈다

지도교수 : 최홍석

공동 지도 교수: 오 원 근

약학과

조선대학교 대학원

PEDV 바이러스에 의한 돼지에서 일어나는 질병은 돼지를 기르는 축산에서 설사를 야기하는 질병을 일으켜, 축산업의 생산성에 심각한 손실을 야기한다. PEDV 바이러스를 저해하는 화합물을 발굴하기 위하여 국내 자생식물 추출물에 대한 탐색을 실시하여, 후보식물로 방풍(*Saposhnikovia divaricata*, Apiaceae)을 선정하였다.

방풍을 메탄올로 추출한 뒤 농축하여 용매분획을 실시하여 활성을 측정하고 결과 PEDV에 대한 저해활성을 보여주는 물질이 EtoAc 층에 있음을 확인하였다. 이후, EtoAc 분획물을 PEDV에 대한 저해활성을 측정하며, 활성물질을 추적하는 방법으로 크로마토 그래피 기법을 사용하여 화합물을 분리하였다. 분리한 화합물 (1-10)의 화학적 구조를 NMR 방법 등을 이용하여 구조 결정하였다. 이후 분리한 화합물 각각에 대하여, 바이러스를 숙주세포에 감염시키고 바이러스에 의한 세포의 사멸사 저해 정도를 측정하는 방법인 cytopathic effect (CPE) 실험을 실시하여 각 화합물의 항 바이러스

스 활성을 측정하였다. 분리된 화합물 중 화합물 2는 화합물은 VERO 세포에 PEDV 유도된 cytopathic 효과에 대해 상당한 저해 활성을 가지고 있는 것으로 밝혔다. 분리된 다른 화합물들인 화합물 1, 3-5번 화합물도 PEDV에 대한 저해활성을 갖고 있지만 높은 농도에서는 세포독성을 갖음을 확인하였다.

# ABSTRACT

## **Coumarins from radix *Saposhnikovia divaricata* inhibit porcine epidemic diarrhea (PED) virus**

Sharma Govinda

Advisor: Prof. Choi Hong Seok, Ph.D.

Co-Advisor: Prof. Oh Won Keun, Ph.D.

Department of Pharmacy,

Graduate School of Chosun University

The epidemic of PED is grave threat to the swine based agro-economy world-wide and the prophylactic defenses against it are not dependable while there are no agents to treat the infection. This scenario demands for the research to find the solution to this problem. To find the safe, effective and efficient treatment for this virus infection, a plant, *Saposhnikovia divaricata* (Apiaceae) was chosen, after screening many plant samples. This plant is also a very popular constituent of formulations in Traditional Chinese Medicine. The EtOAc extract from radix of this plant was subjected to bioactivity guided successive chromatographic fractionation, using CPE inhibition based antiviral assay. This led to the isolation of ten coumarin type compounds (**1 – 10**). Among these, **2** and **6** were found to have significant inhibitory activity ( $EC_{50}$  : 5.91 and 15.26  $\mu$ M respectively) with good safety index (>3.2) against PEDV induced cytopathic effect in Vero cells. Compound **1**, **3**, **4** and **5** however showed activity at remarkably small concentration of but they also showed increased degree of cytotoxicity, while remaining coumarins didn't have significant CPE inhibitory activity.



# 1. Introduction

## 1.1. Porcine Epidemic Diarrhea (PED)

PED is an infectious disease of pigs, characterized by acute diarrhea, resulting in high mortality in neonatal piglets.<sup>1, 2</sup> The virus causing this disease is PED Virus (PEDV), which was first isolated in 1978 and found to highly resemble the previously known transmissible gastroenteritis (TGE) virus, both of which are Coronaviruses but serologically different.<sup>3</sup> TGEV was more virulent and lethal at that time but now, due to the cross immunity gained against TGE by the emergence of less harmful PRRS virus, the PED virus surpassed TGE as a cause of loss in swine economy.<sup>1</sup>

Since Pensaert and de-Bouck reported PEDV for the first time in 1978, millions of pig deaths have been ascribed to this highly pathogenic virus. From that time, it had remained prominent until 1986, as 69 % of the fattening pigs sampled in Belgium, were found to be infected with PEDV. This percentage decreased to 41 % in 1991-1992 and in 1997 no positive results were found. With these data Pensaert had reached a conclusion that the virus circulated less intensively in those years in Europe, while in Asia the prevalence rates were as high as 50 – 95 %.<sup>4</sup>

In 2000 the Department of Veterinary Pathology in Seoul National University, Korea reported 634 cases of PEDV infection among the 1258 cases studied, i.e. almost 50 %. Moreover, their findings show a trend in seasonal pattern in PEDV occurrence with winter (mainly January) showing the highest occurrence.<sup>5</sup> This epizootic pattern of PEDV prevalence has also been confirmed with another report from Italy. There, the epidemic was reported from 2005 to 2006 in 63 herds, where the mortality in piglets was reported to be just 34 %, but in growers and fatteners the morbidity was found to range from 20 to 80 %.<sup>6</sup>

Another outbreak was reported from Thailand in 2009, which spread throughout the country's farrowing barns in 2007, here the piglets mortality was reported to be 100 %.<sup>7</sup> And the most recent PEDV outbreak that has been reported is from China in 2010, which affected more than 10 provinces in southern China killing more than 1,000,000 piglets. And here also 100 % of the piglets had the disease; further most of them acquired it within 7 days and some even within a few hours.<sup>8</sup>

Thus, it can be inferred that the pathogenicity of the PED virus has been continuously increasing over time. And the risk of this infection is now posing substantial risk to the swine industries.

## **1.2. The virus**

A new coronavirus like agent was demonstrated in the feces of piglets from a farm suffering diarrhea outbreak in 1978, which was later confirmed to be the Porcine Epidemic Diarrhea virus (PEDV).<sup>3</sup> It is a positive-sense, single stranded RNA virus of Coronaviridae family in Nidovirales group.<sup>9-11</sup> All of the viruses in Coronavirus family, during their replication procedure, allow changes in their genome by different mechanisms, due to which they continually evolve into new and at times more virulent strains with higher pathogenicity. Despite their diversity, all Coronaviruses share same replication procedure and morphological features, thus, rather than considering just PEDV, the whole family 'Coronavirus' should be considered for developing defenses against them.

### 1.2.1. Coronavirus

Coronavirions are generally spherically shaped pleomorphic particles ranging in diameter from 60 to 220 nm and bear club shaped surface projections spaced widely, giving them the appearance like that of “Crown” from which its name was derived. It contains in its family the viruses as deadly as SARS-CoV in addition to PEDV, TGEV, FCoV, CCoV, BCoV, IBV etc. and have diverse host range like human, pigs, cats, dogs, cattle and chicken respectively. Different Coronaviruses have intermittently being associated with huge human (SARS) or economic loss (TGEV, PEDV).

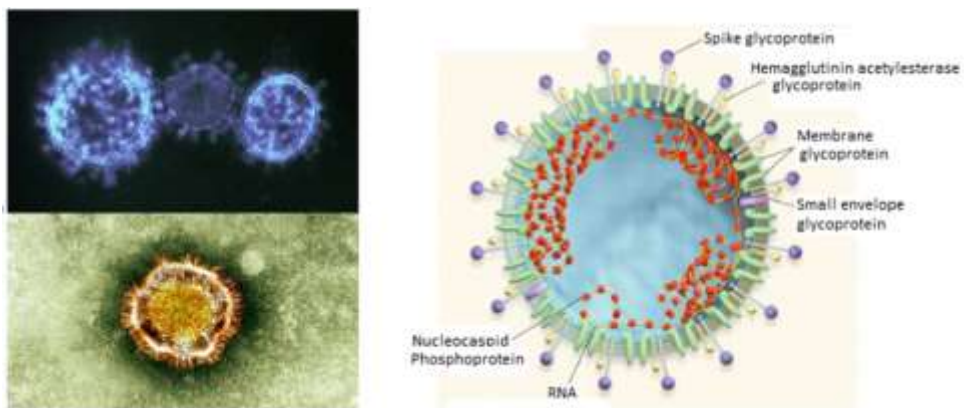


**Figure 1. Microscope photograph and schematic diagram of Coronavirus.** The surface projections of spike proteins give the Coronavirus the “crown” like appearance, which they are named after.

The first Coronavirus, Infectious Bronchitis Virus (IBV), was discovered from chicken embryos in 1937,<sup>12</sup> after which mouse hepatitis virus (MHV) and other mammalian Coronaviruses, including Transmissible gastroenteritis virus (TGEV) in pigs, were isolated in 1940s.<sup>13, 14</sup> Coronaviruses are enveloped viruses, with single-stranded positive sense RNA genome about 30 kb in length that has a 5’ cap structure and 3’ polyadenylation tract. In the host cell, at first the 5’ most open reading frame (ORF) of the viral genome is translated into a

large polyprotein which is then cleaved by viral encoded proteases releasing different nonstructural proteins, including an RNA-dependent RNA polymerase, Adenosine Triphosphatase (ATPase) and helicase. These proteins now replicate the viral genome and also generate nested transcripts used in the synthesis of the viral proteins. Transcription-regulating sequences (TRSs) located at the 5' end of each gene represent signals which are used to regulate the discontinuous transcription of sub-genomic mRNAs.

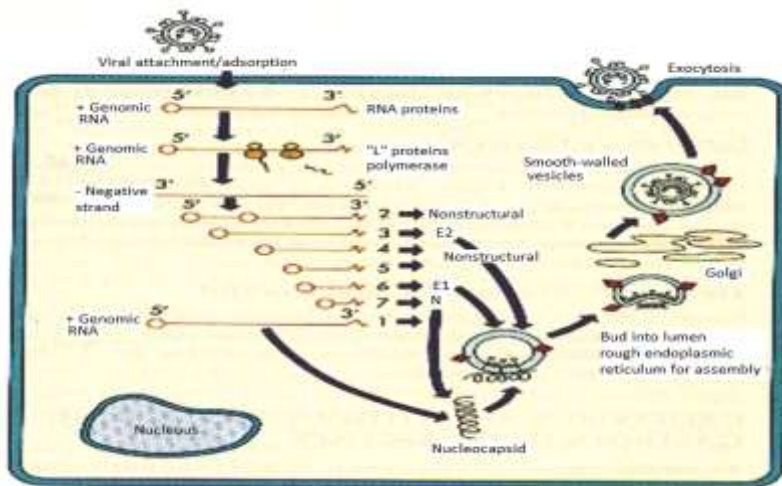


**Figure 2. Replication machinery of Coronavirus**

Although coronavirus family was previously believed to be monogenic comprising 11 viruses,<sup>15</sup> now this number has already reached 26, and the family of coronavirus has been classified phylogenetically to three groups : group 1(or alpha-coronaviruses), 2 (or beta-coronaviruses) and 3(or gamma-coronaviruses) and subsequent subgroups (Table 1).<sup>16</sup> The first two groups contain nine mammalian Coronaviruses, while the third group contains avian Coronaviruses.<sup>17, 18</sup>

**Table 1. Classification of Coronavirus**

<b>Group</b>	<b>Viruses</b>
Group 1 (Alpha–Coronavirus)	Group 1a PEDV, TGEV, FCoV
	Group 1b HCoV-229E, HCoV-NL63, Bat-CoV 512/2005, Bat-CoV HKU2, Bat-CoV HKU8, Bat-CoV 1A
Group 2 (Beta–Coronavirus)	Group 2a HCoV-OC43, BCoV , PHEV, ECoV, MHV, HCoV-HKU1
	Group 2b SARS-CoV, Bat-SARS-CoV, HKU3
	Group 2c Bat-CoV HKU5
	Group 2d Bat-CoV HKU9
Group 3 (Gamma–Coronavirus)	Group 3a IBV, TCoV
	Group 3b SW1
	Group 3c BuCoV HKU11, ThCoV HKU12, MuCoV HKU13

Such tremendous rise in diversity of Coronavirus is ascribed to three main reasons. First is the infidelity of RNA-dependent RNA polymerase, which leads to one mutation in every 1000 to 10,000 nucleotides, replicated.<sup>19</sup> The second is random template switching during replication, which is probably mediated by a “copy choice” mechanism as Coronaviruses have a large number of homologous RNA recombination,<sup>20</sup> and third is its ability to accommodate and modify genes as it possesses the largest known genome among all known RNA viruses. Such high potential for further increase in diversity due to mutation may lead to zoonotic outbreak of Coronavirus with disastrous results.

### 1.2.2. Evolution

After finding the bat-SARS-CoV in 2005, the further studies on bats confirmed 103 different Coronaviruses until 2009.<sup>16, 21</sup> Along with bats, the bird species are also speculated to be reservoirs of Coronaviruses, allowing for wide range of cell types owing to the huge diversity in species of bats and birds. Their extensive migration potential allows for possible exchange of genetic materials with various viruses in wide range of hosts, thus leading to homologous and heterologous recombination along with interspecies jumping, resulting in continuous evolution into a range of different viruses.

Recently, a new Coronavirus named ‘human beta-Coronavirus’ has been reported from Middle east, which causes severe pneumonia and often kidney failure.<sup>22, 23</sup> Consequently the mortality rate after this virus infection has been 50 %, however it is not found to spread easily between human.<sup>24</sup> But, the mutation capabilities of this Coronavirus into swiftly transmissible one like SARS or PEDV should be taken into consideration before underestimating its potential to evolve into a pandemic with tremendous fatalities leading to human and/or economic loss from domesticated animals.

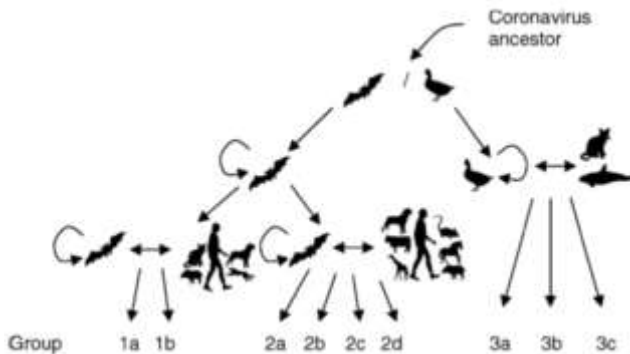


**Figure 3. Evolution of Coronaviruses.** Bats and birds are believed to be the reservoirs, from which the different viruses evolve as a result of homologous and heterologous recombination along with interspecies jumping.

### **1.2.3. Porcine epidemic diarrhea virus (PEDV)**

PEDV falls in alpha-coronavirus genus of Coronaviridae family in Nidovirales group. It contains single stranded positive sense RNA of about 28 kb. Previously it was believed that there is only one strain of PEDV. But according to recent reports there are many strains of PED viruses, varying in their infectivity and genetic constitution, for example the strain found in Korea as well as China are genetically different and more pathogenic from those found in Europe. This probably explains the difference in severity of this disease between Asia and Europe, with higher incidence and severity in the former and indeed a continued evolution leading to new and possibly more virulent strains.<sup>5, 25, 26</sup> Genetic sequence of these viruses has already been worked out including the ORFs encoding the spike proteins, which are believed to be responsible for the pathogenic symptoms.<sup>27</sup> Further, the functional receptor on the cell for this virus has been found to be Porcine aminopeptidase N.<sup>18</sup>

This virus is transmitted predominantly via fecal-oral route, however transmission from sows to piglets via milk has also been reported recently.<sup>8</sup> After the infection, symptoms like watery diarrhea, vomiting/regurgitation and anorexia can be seen in mild cases, while in more severe cases pyrexia, dehydration and signs of abdominal pain can be seen.

## **1.3. Vaccines**

There had been many efforts to formulate a safe and efficient vaccine against PEDV.<sup>28</sup> The live attenuated virus and the gene containing Spike protein sequences are being tested as vaccines.<sup>29, 30</sup> The DR13 strain of live PED virus attenuated by serial passage in Vero cells have been licensed in Korea for prophylaxis against PEDV in pigs.

Spike protein (or S protein), the club shaped projections on the surface of the virus (figure 1) is a type I glycoprotein and contains 1,383 amino acids.<sup>31</sup> Similar to the other members of Coronavirus family, the S protein in PEDV is a glycoprotein peplomer- a surface antigen,<sup>32</sup> and elicits a strong antibody response.<sup>33</sup> In addition, it is also responsible for mediating viral entry by interaction with the host cell's receptors.<sup>34</sup> Thus, it is used as a primary target for the development of vaccines against PEDV.

Although the vaccines have been continually developed but their efficacy has not been found to be satisfactory. The efficiency of such vaccines were reported to be just 50 % even at a very high dose.<sup>2</sup> In Korea DR13 strain attenuated PEDV, licensed as vaccine against PEDV, is in use but the results are not satisfactory.<sup>35</sup> Further, just vaccine or another preventive measure is not sufficient to have a total control over a disease with consequences of disastrous magnitude; in addition to vaccines and preventive measures the solutions to post infection condition need to be researched.

#### **1.4. *Saposhnikovia divaricata* (Apiaceae)**

*Saposhnikovia divaricata* (Fig 3) traditionally known as Fang-feng, is one of the important constituent of many formulations popular in Traditional Chinese Medicine (TCM). It is mainly grown in Heilongjian, Jilin and Liaoning provinces of China, and also in some parts of Korea, Mongolia, Russia and USA. The root is generally collected in spring and autumn then they are sliced and dried in sunlight and consumed alone or in combination with other plants as per the traditional formulae. According to the traditional Chinese system of medicine, it is believed to dispel the “wind” related syndromes, the indications and formulations of which have been compiled in Chinese Material Medica.<sup>36</sup>



In TCM pernicious influence of wind is believed to be one of the major causes of illness due to disharmony among the elements in human body. It can combine with other pathogens and results in the range of syndromes like, ‘wind cold’, ‘wind heat’ and ‘wind dampness’. These syndromes often attack the upper part of the body, head, throat, eyes etc. Like the moving nature of wind the symptoms associated also have moving nature like twitching, spasms or shaking. The ‘external wind’ often affects mind whereas the ‘internal wind’ is related to imbalances in the liver. For treating such and other syndromes it is often used in combination with *Henthae*, *Folium mori*, *Herba schizonepetae*, *Fructus arctii*, *Fructus tribuli* etc.

**Classification:**

Kingdom : Plantae  
Division : Magnoliophyta  
Class : Magnoliopsida  
Order : Apiales  
Family : Apiaceae  
Genus : *Saposhnikovia*  
Species : *divaricata*

Various uses of this plant documented in Chinese Materia Medica are measles, pruritus, tetanus, opisthotonos, convulsions, spasms and cold among others.<sup>36</sup> Coumarins, pyrano coumarins and chromones, which have a wide range of biological activities, are reported to be constituents of this plant. Previously the chromones like prim-O-glucosylcimifugin, 5-O-methylvisammioside,<sup>37</sup> cimifugin,<sup>38</sup> and sec-O-glucosylhamaudol<sup>39</sup> etc. were reported as major and bioactive constituents of this plant, and subsequently various

methods for optimizing their isolation yield has been studied.<sup>40, 41</sup> Various compounds of this plant have been studied for their bioactivity in different areas.

Chromones like divaricatol, ledebouriellol and hamaudol were confirmed to be the analgesic components, while radix *S. divaricata*'s ethanol extract was found to have anti-proliferative activity against human tumor cell lines. Further, these constituents were found to have potent anti-oxidant and anti-inflammatory activities in the nontoxic concentrations.<sup>42, 43</sup> A formula consisting of *S. divaricata* which is popular in Asia as traditional solutions for treatment of neuropathic and inflammatory disease, has also been found to exert protective effect against peripheral nerve injury in rats<sup>44</sup>. In addition to aforementioned traditional indications, it has also been reported to potentiate reticuloendothelial system, which functions as a defense against infections in human body.<sup>45</sup>

In addition to chromones, coumarins are also found in *S. divaricata*. Coumarins constitute a group of polyphenolic secondary metabolites from plants, chemically belonging to benzopyrones family, and possessing wide range of bioactivity. First member of this group was isolated from *Coumarouna odorata Aube* (Tonka beans), from which the group got its name. Until now, more than 1300 coumarins have been identified<sup>46</sup>; most of them are secondary metabolites in plants, fungi and bacteria while many are synthesized. Earlier studies have established that coumarin derivatives have various activities like anti-inflammatory<sup>47, 48</sup> antibacterial,<sup>49, 50</sup> antifungal<sup>51</sup>, anti-cancer<sup>52, 53</sup> etc.

Combinations containing crude *S. divaricata* have been found to inhibit different type of viruses.<sup>54-56</sup> The compounds isolated in this study- the khellactones, previously found from the sources other than this plant, are reported to have antiviral activity against different viruses<sup>57-59</sup>, but no reports of activity of neither this plant nor the Khellactones against PEDV have been reported yet. Thus, in the course of finding anti-viral compounds against PEDV from

natural sources, this plant was considered for study of its constituent's and their anti-viral activity. On the initial screening the EtOAc soluble fraction of methanol extract from this plant's radix showed CPE inhibitory activity against PED virus. Then the extract was fractionated on the basis of bio-activity results leading to the isolation of ten coumarin derivatives (1–10). This thesis describes the isolation, structure elucidation and results of anti-viral activity assessment of these isolates against PEDV along with the evaluation of associated cytotoxicity and related structure activity relationship.



**Figure 4. *Saposhnikovia divaricata* - 1. Root with branch; 2. Branch with flowers; 3. Sliced dry herb.**

## 2. Materials and Methods

### 1.1. Materials

#### 1.2.1. Plant material

Dried radix of *S. divaricata* was purchased in September 2011 from a local market and was identified botanically by Prof. Oh Won Keun and Dr. Trong Tuan Dao. A voucher specimen (CU2011-12) has been deposited at the Herbarium of the Chosun University, Gwangju, Korea.

#### 1.2.2. Chemicals reagents and chromatography

Silicagel (Merck, 63-200  $\mu\text{M}$  particle size), RP-18 (Merck, 40-63  $\mu\text{M}$  particle size) and Sephadex LH-20 were used for column chromatography. TLC was carried out with silica gel 60 F254 and RP-18 F254 plates. HPLC was carried out using a Gibson system with a UV detector and an Optima Pak C18 column (10 x 250 mm, 10  $\mu\text{M}$  particle size, RS Tech, Korea). NMR spectra were obtained on a Varian Inova 500 MHz and 300 MHz spectrometer with TMS as the internal standard at the Korea Basic Science Institute (KBSI, Gwangju Center, Korea). All solvents used for extraction and isolation were analytical grade. The EIMS data was measured on a Micromass QTOF2 (Micromass, Wythenshawe, UK) mass spectrometer.

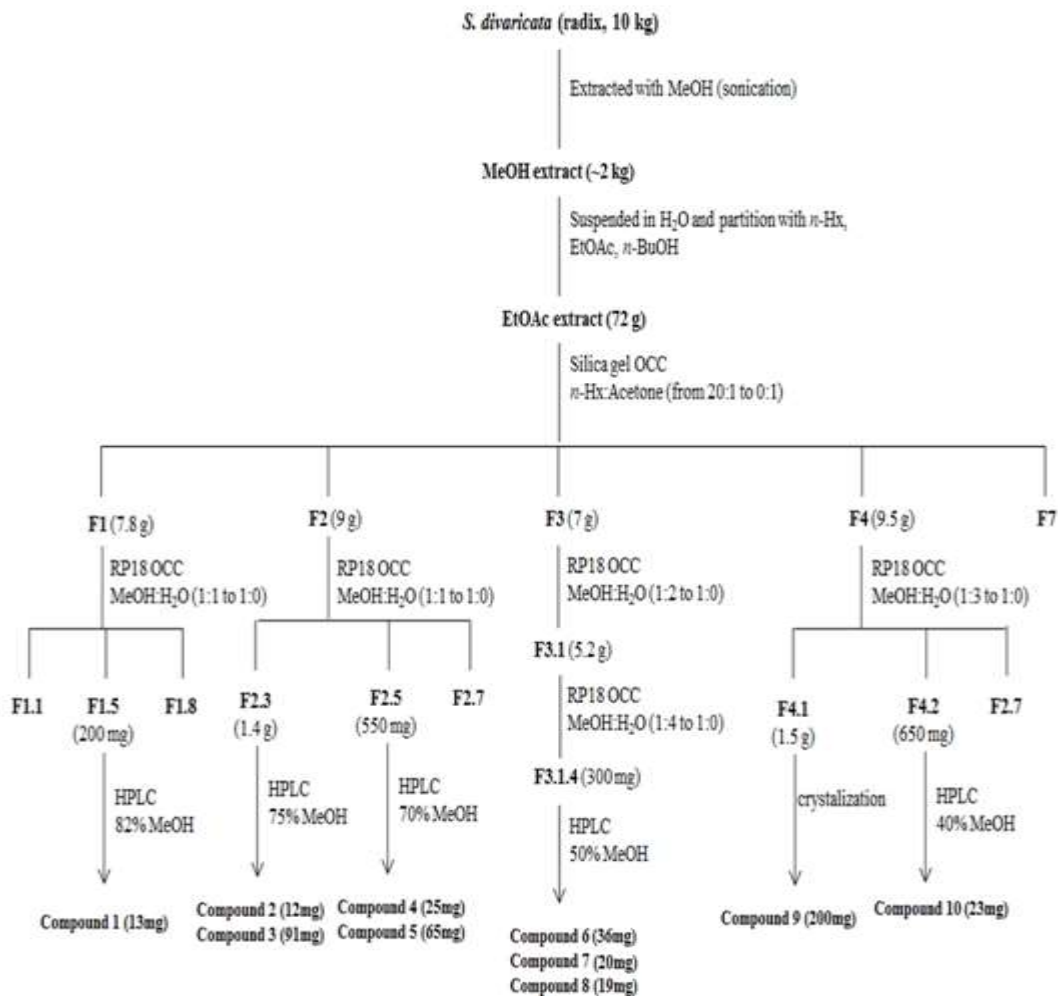
Ribavirin and Glycyrrhizin were purchased from Sigma Chemical Company (St Louis, MO, USA). Dulbecco's modified Eagle's medium (DMEM), fetal bovine serum (FBS), and trypsin were purchased from GIBCO-BRL (Grand Island, NY, USA). MTT [3-(4,5-dimethylthiazol-2-yl)-2,5-diphenyltetrazolium bromide] was purchased from Sigma, Korea.

## 1.2. Methods

### 1.2.1. Extraction and Isolation

Ten compounds (**1-10**) were isolated using Bioassay-guided fractionation. The dried radix of *Saposhnikovia divaricata* (10kg) was extracted with MeOH using sonication (500 mL x 3 times x 2hrs). Then the obtained methanol extract was filtered and concentrated (2kg), thereafter it was suspended in water and partitioned with Hexane, EtOAc and Butanol (each 2 L X 5 times) yielding 4 fractions. The EtOAc soluble fraction (72g) was found to be most active among all fractions, so it was further fractionated using NP silica gel open column chromatography (10 X 30 cm; 63 – 200 µm particle size) using a gradient of hexane:acetone (from 20:1 to 0:1), to yield seven combined fractions according to their TLC profiles (F1 to F7). Fraction 1 (7.8gm) was subjected to reversed phase C18 (RP-18) open column chromatography (3 X 30 cm; 40-63 µg/mL) and eluted with MeOH:H<sub>2</sub>O (1:1 to 1:0, 1L for each step) to yield 8 sub-fractions (F1.1 to F1.8). Further purification of F1.5 (200mg) by semi-preparative Gilson HPLC systems [using RS Tech Optima Pak C18 column (10 X 250 mm, 10µm particle size); mobile phase MeOH:H<sub>2</sub>O (82:18); flow rate 2mL/min; UV-detection at 205 and 254 nm] resulted in the isolation of **Compound 1**(13mg; t<sub>R</sub> = 24 min ). Similarly, fraction 2 (9g) was also subjected to reverse phase open column chromatography (RP-18) with mobile phase MeOH:H<sub>2</sub>O (1:1 to 1:0) and fractionated to seven sub-fractions (F2.1 to F2.7). Then the sub-fraction F2.3(1.4g) was further purified using Gilson HPLC system [RS Tech Optimapak C18 column (10 × 250 mm, 10 µm particle size); eluted with 75% methanol in water with flow rate 2 mL/min; UV-detection at 205 and 254 nm] leading to the isolation of **Compound 2** (12mg; t<sub>R</sub> = 27 min) and **compound 3** (91mg; t<sub>R</sub> = 42.5 min) respectively. Also, the sub-fraction F2.5 (550mg) was purified using Gilson HPLC system [RS tech

OptimapakC18 column (10 × 250 mm, 10 μm particle size); eluted with MeOH:H<sub>2</sub>O (7:3) and flow rate 2mL/min; UV-detection at 205 and 254 nm] leading to the isolation of **Compound 4** (25mg; t<sub>R</sub> : 35 min) and **compound 5** (65 mg; t<sub>R</sub> :48 min). Fraction 3 yielded three compounds **6**, **7** and **8** (36, 20 and 19 mg with t<sub>R</sub> 34, 33, and 35.5 min respectively) upon chromatographic fractionation using RP18 (MeOH:H<sub>2</sub>O- 1:2 to 1:0) subsequently applying the sub-fraction 3.1 to the RP18 open column (MeOH:H<sub>2</sub>O- 1:4 to 1:0) and finally purifying the sub-fraction 3.1.4 using HPLC [RS Tech Optimapak C18 column (10 × 250 mm, 10 μm particle size; flow rate of 2mL/min; UV-detection at 205 and 254 nm)] with 50% MeOH. The fraction 4 yielded 7 sub-fractions(4.1 to 4.7) after applying to RP 18 open column with solvent system of MeOH:H<sub>2</sub>O(1:3 to1:0). The compound **9** (200 mg)was isolated by crystallization from the first sub-fractionF4.1(1.5 g), and **compound 10** (23mg),was isolated from sub-fraction F4.2(650 mg) by using HPLC system with 40 % MeOH as mobile phase[RS Tech Optimapak C18 column (10 × 250 mm, 10 μm particle size;flow rate of 2mL/min; UV-detection at 205 and 254 nm)].



**Scheme 1. Isolation scheme of compounds from radix of *S. divaricata***

## **1.2.2. Viruses and cell**

The Porcine Epidemic Diarrhea Virus (PEDV) (CV777) kindly provided by Choong Ang Vaccine Laboratory, was used in this study. Vero (African green monkey) cells (ATCC CCR-81) were maintained in Dulbecco's Modified Eagle's Medium (DMEM) (Gibco) supplemented with 10% fetal bovine serum at 37°C and 5 % CO<sub>2</sub>. The virus stock was stored in -80°C, for infection it was thawed in room temperature and suspended in 37°C DMEM before infecting the cells.

## **1.2.3. Cytopathic effect (CPE) inhibition**

### **2.2.3.1 Cytopathic effect**

After infecting the susceptible cell, the virus induces some morphological changes, like enlarged vacuoles, syncytium formation usually leading to death in the host and surrounding cells, this visible effect is called cytopathic effect.<sup>60</sup> It is used to evaluate the pathogenicity of the virus during in-vitro cell based experiments. Conventionally, the CPE assay procedures are read by staining the cells after the CPE is induced by the virus. This procedure requires the manual counting of the no. of plaques under microscope, which can be seen as unstained patches in the monolayer of cells. A number of replicates need to be performed, and visual counting of the plaques is a labor intensive task, further the results are bound contain a degree of error due subjective microscopic interpretation. Automated methods of counting plaques in such experiment have also been described.<sup>61</sup> But such methods are expensive due to obvious reasons. Another type of assay which utilizes tetrazolium salt (MTT), for evaluating the gross percentage of live cells after the virus infection is more appropriate, as



the results are free of subjective error. This assay was used as previously described with slight modifications for evaluation of CPE inhibition effect of the compounds in this study.<sup>62</sup>

### **2.2.3.2 CPE inhibition assay**

5000 Vero cells per well were seeded in 96 well plate, then they were infected with PEDV virus diluted to 4.4 TCID<sub>50</sub> concentration for 1hr in 37°C with humidified 5% CO<sub>2</sub> atmosphere. After that, the compounds were treated at different concentrations and further incubated for 4 days. The virus and medium control also were maintained and experiment for each dilution was performed in triplicate. After 4 day of incubation, 4 mg/mL MTT ((3-(4,5-Dimethylthiazol-2-yl)-2,5-diphenyltetrazolium bromide) was added and further incubated for 4 hrs in same conditions. During this time, the cells unaffected from CPE will uptake the MTT and convert it into deep blue formazan crystal by the action of their mitochondrial enzyme. To measure the formazan formed, the medium is aspirated and 100 µL DMSO is added and allowed to dissolve the formazan by shaking for 2 min. Then the absorbance is measured at 550 nM. The experimental values are compared with medium control, where instead of virus just media was added; value of this experiment is considered as 100 % CPE inhibition, and with respect to this value the experimental values are calculated as mentioned in MTT assay described later.

In the CPE assay procedure, the results are interpreted as the % CPE inhibition, which is correlated from the % of viable cells at the end of the experiment. Since, the cells were infected with virus, they would die due to CPE but if the treated compounds have antiviral effect then cells should not die. Thus, higher percentage cell survival is recognized as higher antiviral activity. However, if the treated compounds themselves are cytotoxic, then cell death due to virus induced CPE and the cytotoxicity of compounds cannot be differentiated. Thus,

those compounds which have antiviral activity at lower concentration but exert cytotoxicity at higher concentration tend to show a peak activity at a certain concentration. This is considered as the optimum concentration. In the case of compound **1**, **3**, **4** and **5** the optimum concentration and resulting % inhibition is shown. (Fig. 42)

### **2.2.3.3 TCID<sub>50</sub> (50 % Tissue culture infectious dose)**

To estimate the virulence of the stock virus suspension, and to maintain the uniformity of virus challenge in the subsequent experiments TCID<sub>50</sub> was determined by using the CPE based assay previously described with slight modifications.<sup>62</sup> In a 96 well plate, 5000 vero cells/well were infected with different dilutions of the stock virus suspension, ranging from 1: 50 to 1: 3200 with two fold serial dilution. After 4 days of incubation in 37°C with 5 % CO<sub>2</sub> atmosphere, percentage of cells surviving the viral cytopathic effect was measured with MTT based assay. The mean values of three experiments with ± standard deviation percentage was calculated. Finally, regression analysis was performed to calculate the 50 % tissue culture infectious dose.

### **1.2.4. MTT assay**

This assay was used to estimate the cytotoxicity of the compounds in the Vero cells. It is based on the conversion of yellow water soluble substrate 3-(4,5-dimethylthiazol-2-yl)-2,5-diphenyl tetrazolium bromide (MTT) into a dark blue formazan by the mitochondrial dehydrogenase enzyme in living cells. In dead cells this enzyme being not functional, only living cells can form the formazan crystals from the MTT. These formazan crystals can be

dissolved in DMSO and shows absorbance at 250 nm wavelength. Thus allowing us to estimate the alive cells in an experiment.

5000 Vero cells were seeded in each well of the flat bottom 96 well plate, and incubated for 1 hr. Then, the compounds in different concentrations were treated to the cells, and just vehicle was treated for control. Each experiment was performed in triplicate.

After, 4 days of incubation in 37°C with 5 % CO<sub>2</sub> atmosphere, 2mg/mL MTT reagent was treated and further incubated for 4 hrs and then all the media was aspirated, after which 100 µL DMSO was added. After shaking for about two minutes absorbance of the individual well was measured using VersaMax™ Absorbance Microplate Reader at 540 nM. The vehicle treated well absorbance values were considered as 100 % cell viability (i.e. 0% cytotoxicity), and other experiment values calculated as follows:

$$\% \text{ Cell viability} = \frac{\text{experiment absorbance}}{\text{Control absorbance}} \times 100$$

### **1.2.5. Statistical analysis**

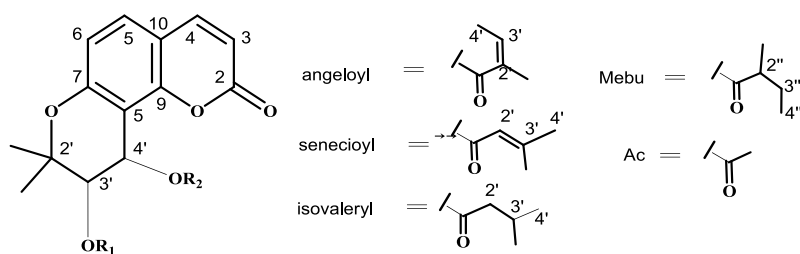
Results are interpreted as mean ± SD of the experiments performed in triplicate. The IC<sub>50</sub>, TCID<sub>50</sub> and CC<sub>50</sub> were calculated by regression analysis using Sigmaplot 11.0 software.

### 3. Results and Discussions

#### 1.1. Isolation of compounds from radix of *S. divaricata*

Total 10 compounds (**1** to **10**) were isolated from the dried radix of *Saposhnikovia divaricata*, by bioactivity guided fractionation using various successive chromatographic and other techniques like crystallization.

#### 1.2. Structures of isolated compounds



- 1 R<sub>1</sub> = angeloyl, R<sub>2</sub> = Mebu
- 2 R<sub>1</sub> = Ac, R<sub>2</sub> = Mebu
- 3 R<sub>1</sub> = R<sub>2</sub> = angeloyl
- 4 R<sub>1</sub> = R<sub>2</sub> = senecieryl
- 5 R<sub>1</sub> = isovaleryl, R<sub>2</sub> = senecieryl
- 6 R<sub>1</sub> = R<sub>2</sub> = H

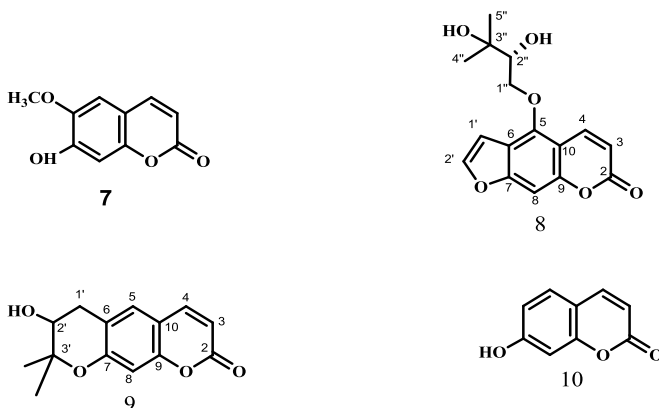


Figure 5. Structure of compounds (**1** to **10**) isolated from radix of *S. divaricata*

### 1.3. Structure determination of isolated compounds

#### 1.2.1. Structure determination of compound 1

Compound **1** (Hyuganin A) was obtained as white powder. Its molecular formula  $C_{24}H_{28}O_7$  was confirmed from the molecular ion peak at  $m/z$  428 ( $M^+$ ) in the EI-MS and by high resolution MS measurement. The  $^1H$ -NMR and  $^{13}C$ -NMR in  $CDCl_3$  spectra of compound **1** (fig. 2 and 3) showed signals assignable to a coumarin moiety [ $\delta$  6.22 (d,  $J=9.5$  Hz, 3-H), 7.59 (d,  $J=9.5$  Hz, 4-H), 7.36 (d,  $J=8.7$  Hz, 5-H), 6.81 (d,  $J=8.7$  Hz, 6-H)], two tertiary methyls [ $\delta$  1.45, 1.48 (both s, 2'-gem- $CH_3$ )], two methines bearing an ester function [ $\delta$  5.40 (d,  $J=4.8$  Hz, 3'-H), 6.61 (d,  $J=4.8$  Hz, 4'-H)], an angeloyl group [ $\delta$  6.12 (m, 3''-H), 1.97 (d,  $J=7.2$  Hz, 4''-H), 1.88 (s, 5''-H)], and a 2-methyl-butyroyl group [ $\delta$  2.38 (ddq,  $J=7.0, 7.0, 7.0$  Hz, 2'''-H), 1.43 (m, 3'''-H), 1.72 (m, 3'''-H), 0.9 (t,  $J=7.5$  Hz, 4'''- $H_3$ ), 1.19 (d,  $J=7.0$  Hz, 5'''- $H_3$ )]. The EI-MS data of **1** showed the fragment ion peaks at  $m/z$  328, 313, 244, 229, 85 and 83, which were derived by eliminations of the angeloyl and 2-methylbutyryl groups.

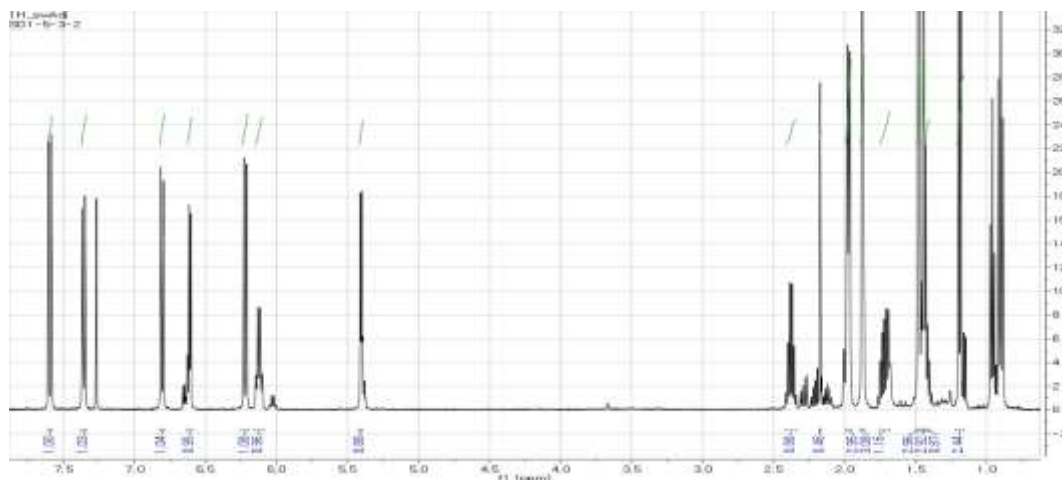
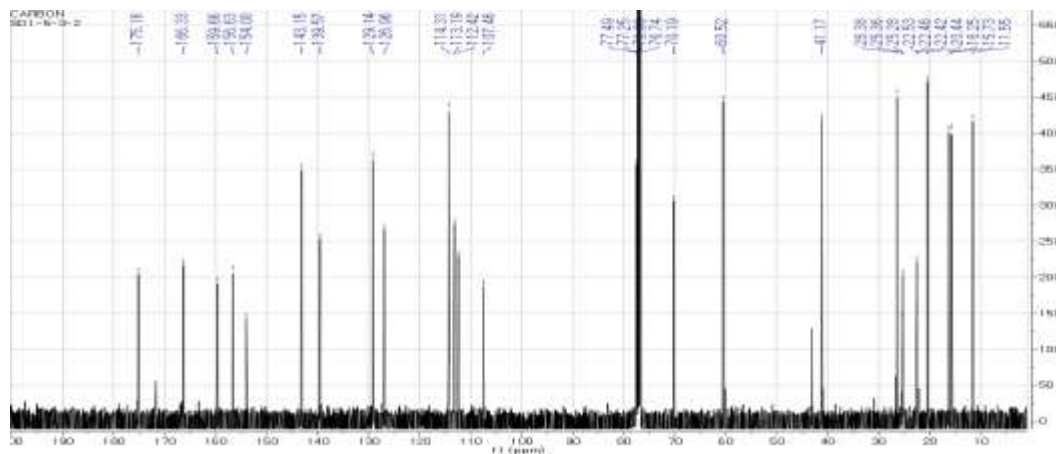
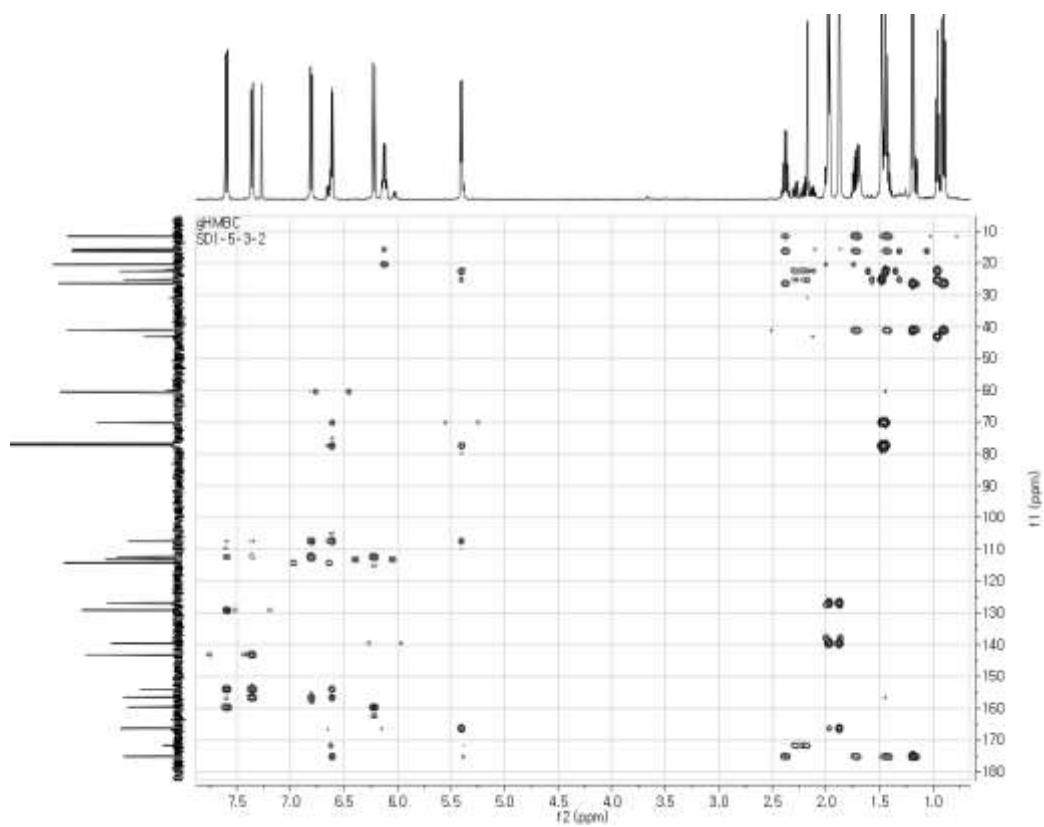


Figure 6.  $^1H$ -NMR spectrum of compound **1** (500 MHz,  $CDCl_3$ )



**Figure 7.**  $^{13}\text{C}$ -NMR spectrum of compound 1 (125 MHz,  $\text{CDCl}_3$ )

The position of angeloyl and 2-methylbutyroyl groups in 1 was clarified by HMBC experiment, which showed a long-range correlation between the 3'-proton and the 1-carbonyl carbon of the angeloyl group and between the 4'-proton and the 1-carbonyl carbon of the 2-methylbutyroyl group as shown in the Figure 10. The configurations of the 3' and 4'-positions in compound 1 were deduced to be cis-orientation on the basis of the coupling constant ( $J=4.8$  Hz) between the 3' and 4'-proton in the  $^1\text{H}$ -NMR spectrum of 1. On the basis of this evidence, the structure of 1 was elucidated as Hyuganin A.<sup>63</sup>



**Figure 8. HMBC spectrum of Compound 1**

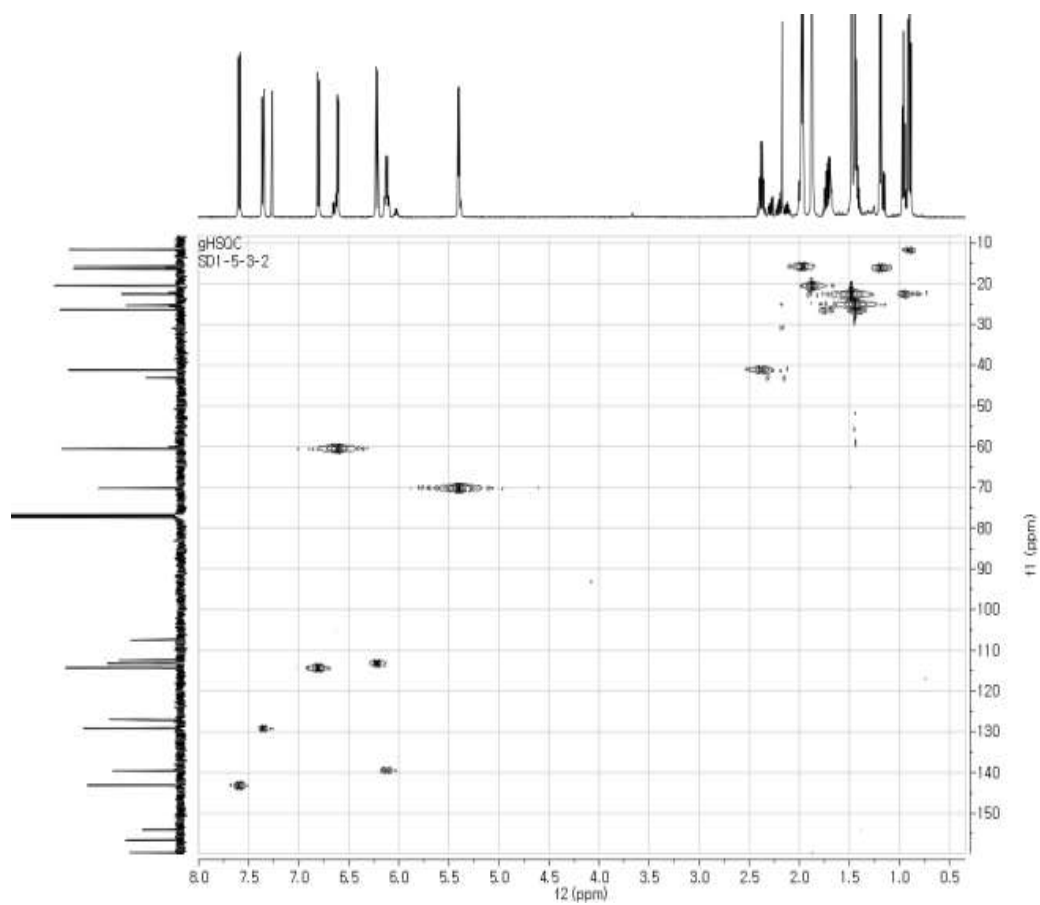


**Figure 9. HSQC spectrum of compound 1**



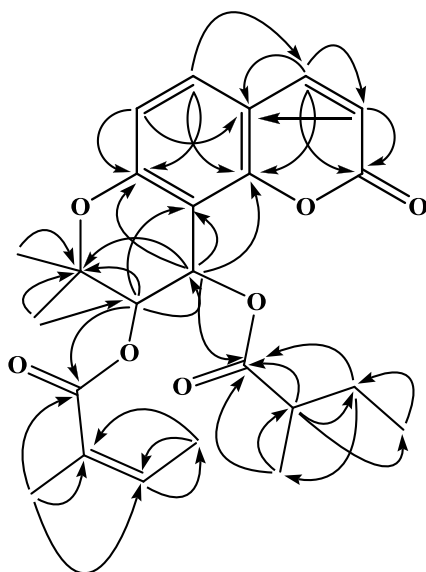


**Figure 10. Key HMBC [H (solid arrow) C] Correlations for compound 1**

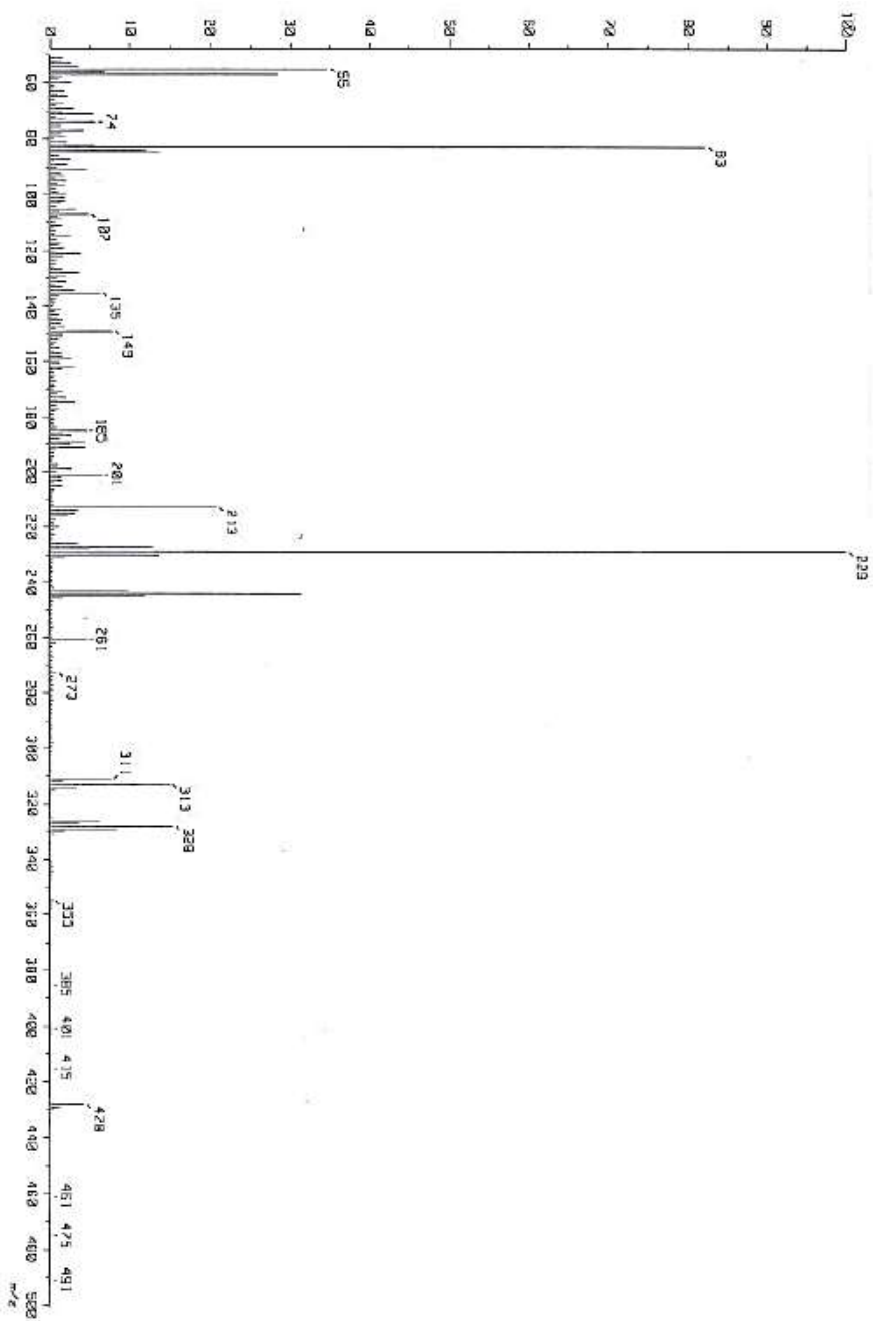


Figure 11. Low resolution EI-Mass Spectrum for compound 1

## 1.2.2. Structure determination of compound 2

Compound **2** was purified as a white powder, with the molecular formula  $C_{21}H_{24}O_7$ . The  $^1H$ -NMR and  $^{13}C$ -NMR (Acetone- $d_6$ ) spectra of compound showed the presence of a cis-khellactone moiety [ $\delta$  6.22 (d,  $J=9.5$  Hz, 3-H), 7.91 (d,  $J=9.5$  Hz, 4-H), 7.59 (d,  $J=8.6$  Hz, 5-H), 6.84 (d,  $J=8.6$  Hz, 6-H), 1.43, 1.44 (both s, 2'-gem- $CH_3$ ), 5.26 (d,  $J=4.8$  Hz, 3'-H), 6.49 (d,  $J=4.8$  Hz, 4'-H)], an acetyl group [ $\delta$  2.03 (s, 2''- $H_3$ )] and a 2-methylbutyryl group [ $\delta$  2.3 (m, 2'''-H), 1.42 (m, 3'''-H), 1.71 (m, 3'''-H), 0.92 (m, 4'''- $H_3$ ), 1.14 (d,  $J=7.0$  Hz, 5'''- $H_3$ ). The carbon signals in the  $^{13}C$ -NMR spectrum of compound **2** were shown to be superimposable on those of compound **1**, except for some signals assignable to an acyl group at the 3'-position. Thus, compound **2** was determined to be Hyuganin C.<sup>63</sup>

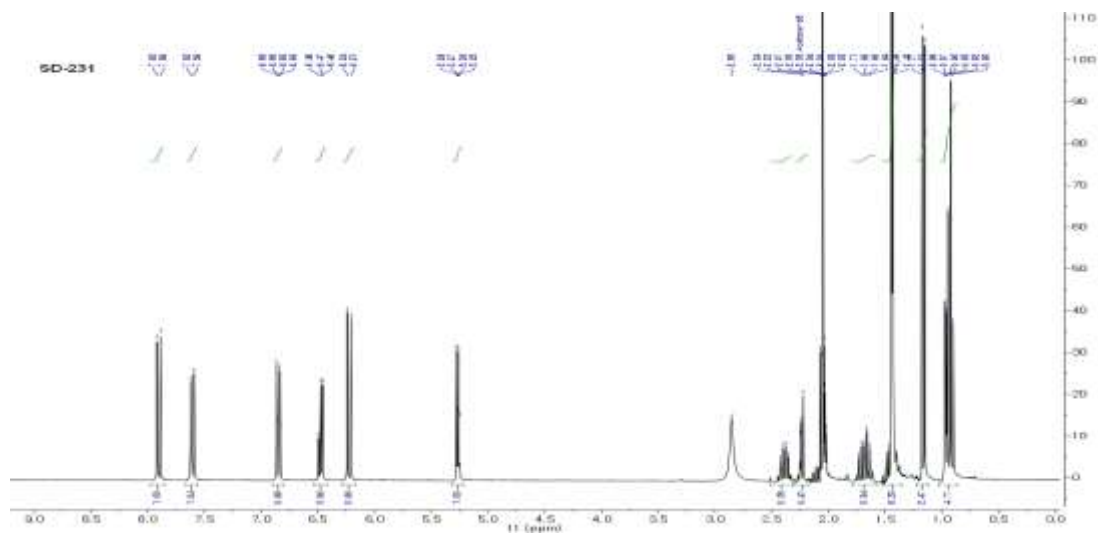
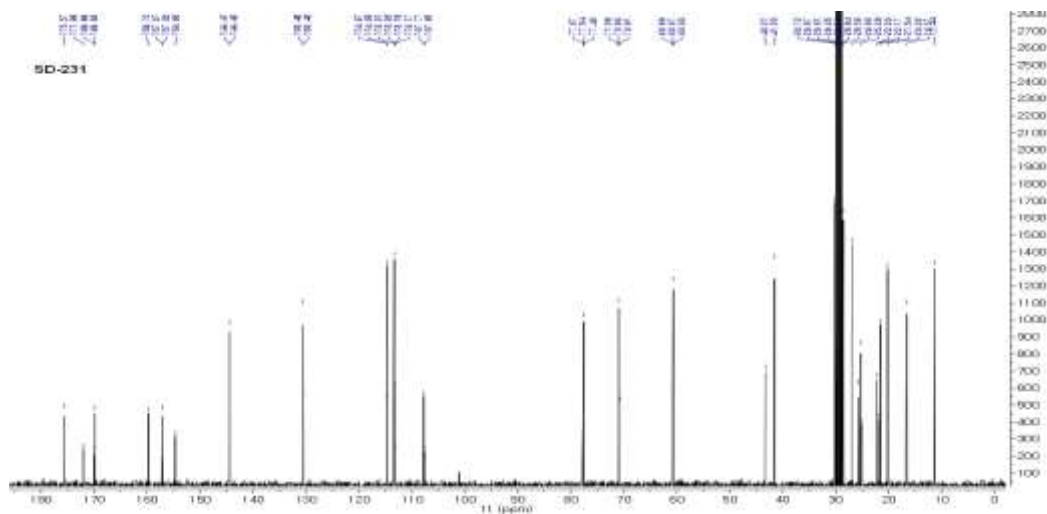


Figure 12.  $^1H$ -NMR spectrum of compound **2** (300 MHz, Acetone- $d_6$ )



**Figure 13.**  $^{13}\text{C}$ -NMR spectrum of compound **2** (75 MHz, Acetone- $d_6$ )

### 1.2.3. Structure determination of compound **3**

Compound **3** was purified as a white powder, with the molecular formula  $\text{C}_{24}\text{H}_{26}\text{O}_7$ . The  $^1\text{H}$ -NMR and  $^{13}\text{C}$ -NMR (Acetone- $d_6$ ) spectra of compound showed the presence of a *cis*-khellactone moiety [ $\delta$  6.17 (d,  $J=9.5$  Hz, 3-H), 7.82 (d,  $J=9.5$  Hz, 4-H), 7.54 (d,  $J=8.6$  Hz, 5-H), 6.81 (d,  $J=8.6$  Hz, 6-H), 1.45, 1.48 (both s, 2'-gem- $\text{CH}_3$ ), 5.27 (d,  $J=4.8$  Hz, 3'-H), 6.52 (d,  $J=4.8$  Hz, 4'-H)] and 3'/4' diangeloyl substitution [ $\delta$  5.6 (q, 3''/3'''-H), 1.88 (d,  $J=7.2$  Hz, 4''/4'''-H), 1.97 (s, 5''/5'''-H)]. Therefore, compound **3** was determined as Praeruptorin B (*cis*-3', 4'-diangeloxylkhellactone).<sup>64</sup>

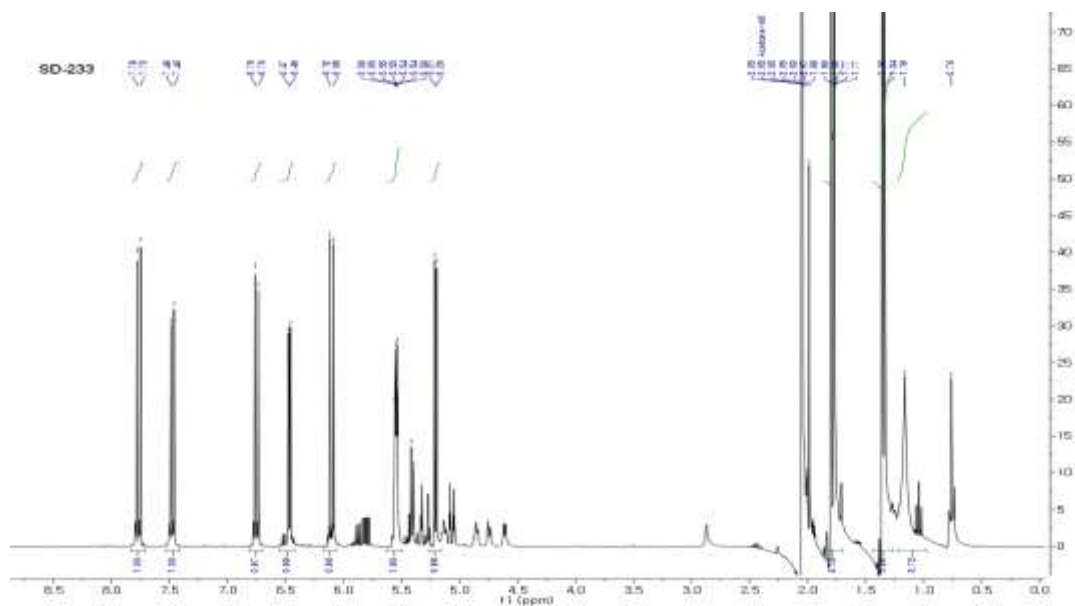


Figure 14.  $^1\text{H-NMR}$  spectrum of compound 3 (300 MHz, Acetone- $d_6$ )

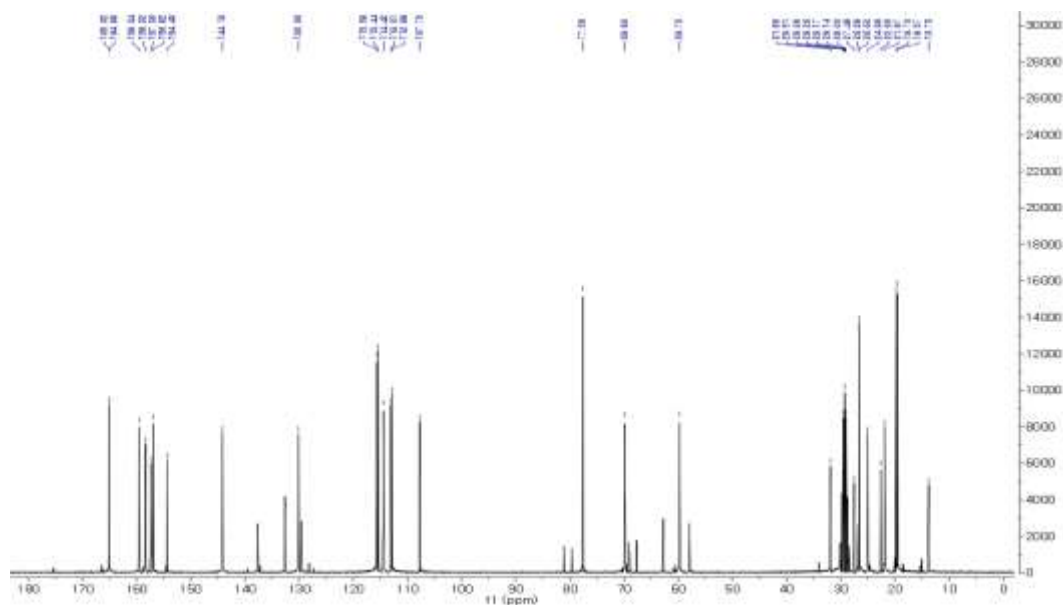


Figure 15.  $^{13}\text{C-NMR}$  spectrum of compound 3 (75 MHz, Acetone- $d_6$ )

**Table 2.**  $^1\text{H}$  and  $^{13}\text{C}$  NMR data for compound **1**, **2** and **3**.

Pos.	1		2		3	
	$\delta_{\text{H}}$ mult.(J in Hz)	$\delta_{\text{C}}$	$\delta_{\text{H}}$ mult.(J in Hz)	$\delta_{\text{C}}$	$\delta_{\text{H}}$ mult.(J in Hz)	$\delta_{\text{C}}$
2		159.7		160.1		160.0
3	6.22 d (9.5)	113.2	6.22 d (9.5)	112.3	6.17 d (9.5)	113.5
4	7.59 d (9.5)	143.1	7.91 d (9.5)	144.8	7.82 d (9.5)	143.5
5	7.36 d (8.7)	129.1	7.59 d (8.6)	128.7	7.54 d (8.6)	129.5
6	6.81 d (8.7)	114.3	6.84 d (8.6)	115.1	6.81 d (8.6)	114.6
7		156.6		157.4		156.9
8		107.5		107.7		107.7
9		154.0		155.0		154.3
10		112.4		112.1		112.7
2'		77.4		79.7		77.4
3'	5.40 d (4.8)	70.1	5.26 d (4.8)	72.3	5.27 d (4.8)	70.4
4'	6.61 d (4.8)	60.5	6.49 d (4.8)	61.4	6.52 d (4.8)	60.7
2'gem	1.45 s	25.4	1.44 s	25.4	1.45 s	25.4
	1.48 s	22.7	1.43 s	21.6	1.48 s	22.7
1''		166.3		170.1		166.7
2''		126.9	2.03 s	20.22		127.2
3''	6.12 m	139.6			5.60 q	139.9
4''	1.97 d (7.2)	15.70			1.88 d (7.2)	15.7
5''	1.88 s	20.4			1.97 s	20.4
1'''		175.6		175.8		166.7
2'''	2.38 ddq (7.0, 7.0, 7.0)	41.2	2.30 m	42.3		127.2
3'''	1.72 m	26.4	1.42 m	27.5	5.60 q	139.9
	1.43 m		1.71 m			
4'''	0.90 t (7.5)	11.6	0.92 m	12.1	1.88 d(7.2)	15.7
5'''	1.19 d (7.0)	16.3	1.14 d (6.9)	17.2	1.97 s	20.4

#### 1.2.4. Structure determination of compound **4**

Compound **4** was purified as white needles, with the molecular formula  $\text{C}_{24}\text{H}_{26}\text{O}_7$ . The  $^1\text{H}$ -NMR and  $^{13}\text{C}$ -NMR (Acetone- $d_6$ ) spectra of compound showed the presence of a cis-khellactone moiety [ $\delta$  6.22 (d,  $J=9.5$  Hz, 3-H), 7.91 (d,  $J=9.5$  Hz, 4-H), 7.59 (d,  $J=8.6$  Hz, 5-H), 6.84 (d,  $J=8.6$  Hz, 6-H), 1.43, 1.44 (both s, 2'-gem- $\text{CH}_3$ ), 5.26 (d,  $J=4.8$  Hz, 3'-H), 6.49 (d,  $J=4.8$  Hz, 4'-H)] and 3'/4' diseneoiyl substitution [ $\delta$  5.61 (br s, 2''/2'''-H), 2.15 (s, 4''/4'''-H), 1.89 (s, 5''/5'''-H)]. Therefore, compound **4** was determined as cis-3',4'-

diseneciolykhellactone.<sup>65</sup>

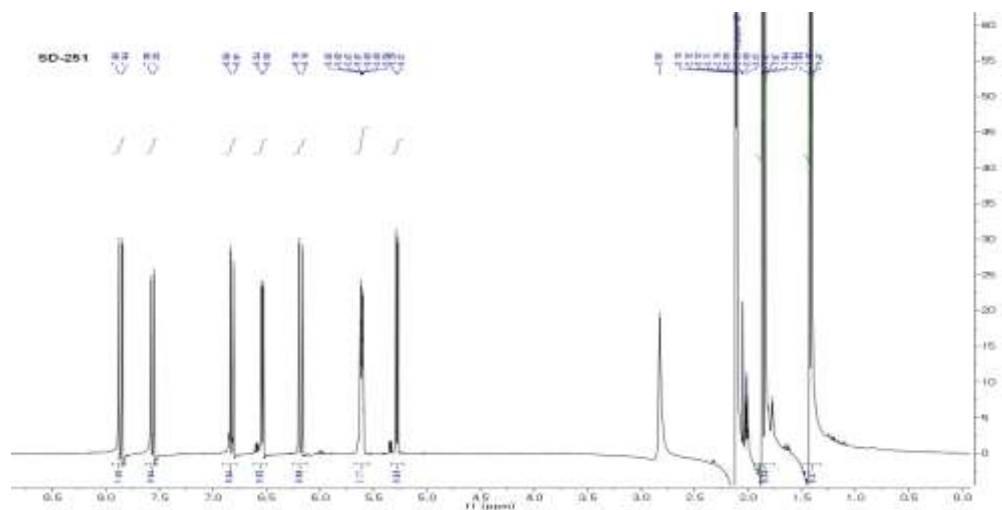


Figure 16. <sup>1</sup>H-NMR spectrum of compound 4 (300 MHz, Acetone-*d*<sub>6</sub>)

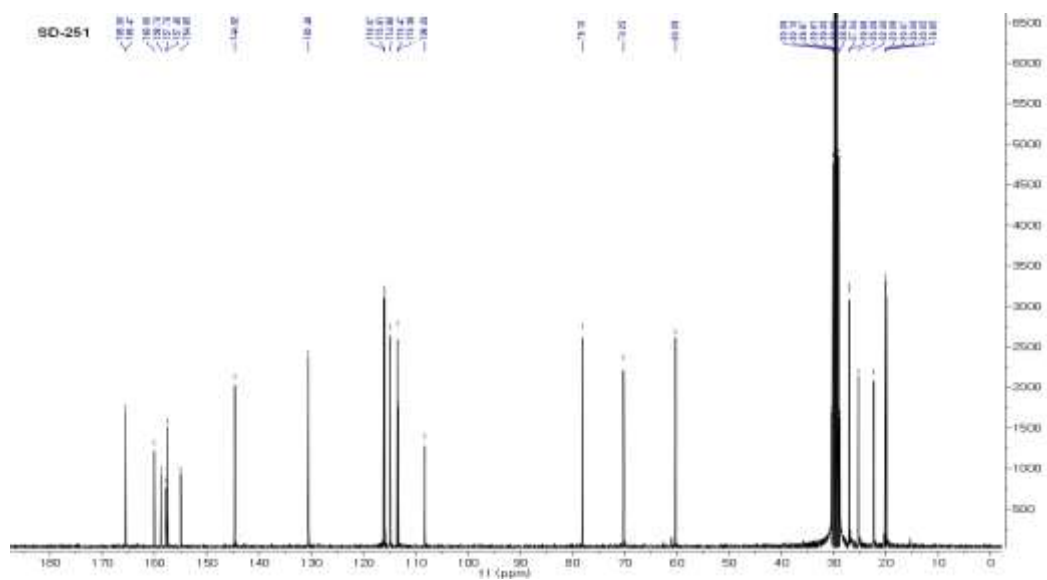


Figure 17. <sup>13</sup>C-NMR spectrum of compound 4 (75 MHz, Acetone-*d*<sub>6</sub>)

### 1.2.5. Structure determination of compound 5

Compound 5 was purified as white powder, with the molecular formula  $C_{24}H_{28}O_7$ . The  $^1H$ -NMR and  $^{13}C$ -NMR (Acetone- $d_6$ ) spectra of compound showed the presence of a cis-khellactone moiety [ $\delta$  6.22 (d,  $J=9.5$  Hz, 3-H), 7.91 (d,  $J=9.5$  Hz, 4-H), 7.59 (d,  $J=8.6$  Hz, 5-H), 6.84 (d,  $J=8.6$  Hz, 6-H), 1.43, 1.44 (both s, 2'-gem- $CH_3$ ), 5.26 (d,  $J=4.8$  Hz, 3'-H), 6.49 (d,  $J=4.8$  Hz, 4'-H)], isovaleryl group [ $\delta$  2.23 (m, 2''-H), 2.15 (m, 3''-H), 0.9-0.94 (m, 4''/5''-6H)] and senecieryl group [ $\delta$  5.61 (br s, 2'''-H), 2.15 (s, 4'''-H), 1.89 (s, 5'''-H)]. Thus, compound 5 was determined as cis-3'-isovaleryl-4'-senecierylkhellactone.<sup>64</sup>

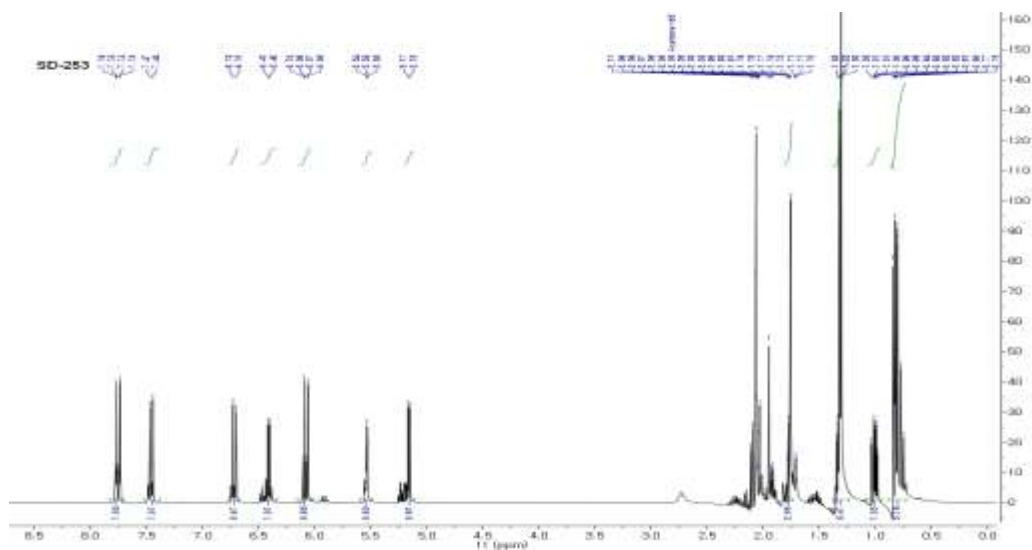


Figure 18.  $^1H$ -NMR spectrum of compound 5 (300 MHz, Acetone- $d_6$ )



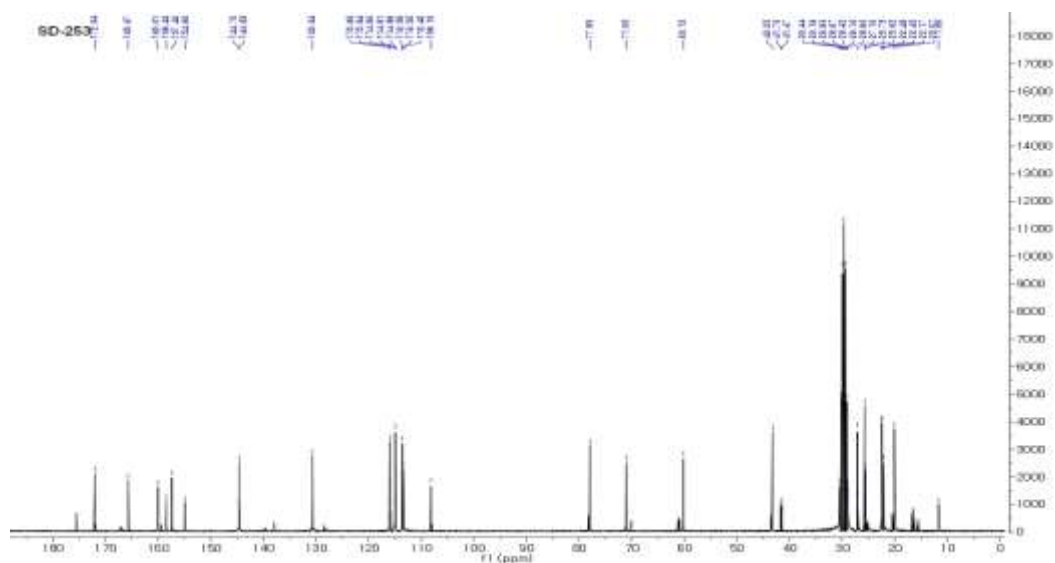


Figure 19.  $^{13}\text{C}$ -NMR spectrum of compound 5 (75 MHz, Acetone- $d_6$ )

### 1.2.6. Structure determination of compound 6

Compound 6 was purified as white powder, with the molecular formula  $\text{C}_{14}\text{H}_{14}\text{O}_5$ . The  $^1\text{H}$ -NMR and  $^{13}\text{C}$ -NMR (Acetone- $d_6$ ) spectra of compound showed the presence of a *cis*-khellactone moiety [ $\delta$  6.20 (d,  $J=9.4$  Hz, 3-H), 7.80 (d,  $J=9.4$  Hz, 4-H), 7.48 (d,  $J=8.5$  Hz, 5-H), 6.75 (d,  $J=8.5$  Hz, 6-H), 1.43 (s, 6H), 3.8 (br s, 3'-H), 5.12 (br s, 4'-H)] with 3'/4' position hydroxyl substitution. The structure of the compound 6 was determined to be *cis*-khellactone.<sup>66, 67</sup>



**Table 3.**  $^1\text{H}$  and  $^{13}\text{C}$  NMR data for compounds **4**, **5** and **6**.

Pos.	4		5		6	
	$\delta_{\text{H}}$ mult.(J in Hz)	$\delta_{\text{C}}$	$\delta_{\text{H}}$ mult.(J in Hz)	$\delta_{\text{C}}$	$\delta_{\text{H}}$ mult.(J in Hz)	$\delta_{\text{C}}$
2	6.22 d (9.5)	160.1	6.22 d (9.5)	160.1	6.20 d (9.4)	161.7
3	7.91 d (9.5)	112.3	7.91 d (9.5)	112.3	7.8 d (9.4)	112.3
4	7.59 d (8.6)	144.8	7.59 d (8.6)	144.8	7.48 d (8.5)	144.6
5	6.84 d (8.6)	128.7	6.84 d (8.6)	128.7	6.75 d (8.5)	128.7
6		115.1		115.1		115.1
7		157.4		157.4		156.7
8		108.28		111.2		111.2
9		155.0		155.0		154.6
10		112.1		112.1		112.1
2'		79.7		79.7		79.7
3'	5.26 d (4.8)	72.3	6.49 d (4.8)	61.4	3.8 brs	72.3
4'	6.49 d (4.8)	61.4	5.36 d (4.8)	72.3	5.12 brs	61.4
2'gem	1.44 s	25.4	1.44 s	25.4	1.43 s	25.4
	1.43 s	21.6	1.43 s	21.6	1.43 s	21.6
1''		165.5		172.4		
2''	5.61 brs	116.2	2.23 m	43.2		
3''		157.8	2.15 m	26.3		
4''	2.15 s	20.2	0.90	22.3		
5''	1.89 s	27.2	0.94	22.3		
1'''		165.6		165.6		
2'''	5.61 brs	116.2	5.61 brs	116.2		
3'''		157.8		157.6		
4'''	2.15 s	20.2	2.15 s	20.2		
5'''	1.89 s	27.2	1.89 s	27.2		

### 1.2.7. Structure determination of compound **7**

Compound **7** was purified as white crystals with the molecular formula  $\text{C}_{10}\text{H}_8\text{O}_4$ . The  $^1\text{H}$ -NMR and  $^{13}\text{C}$ -NMR (Acetone- $d_6$ ) spectra of compound showed the presence of coumarin skeleton [ $\delta$  6.17 (d,  $J=9.5$  Hz, 3-H), 7.85 (d,  $J=9.5$  Hz, 4-H), 7.18 (s, 5-H), 6.74 (s, 8-H)] with 6-position methoxy [ $\delta$  3.94 (s, 6-OCH<sub>3</sub>)] and 7-position hydroxyl group attachment. The structure of the compound **7** was determined to be scopoletin.<sup>68</sup>

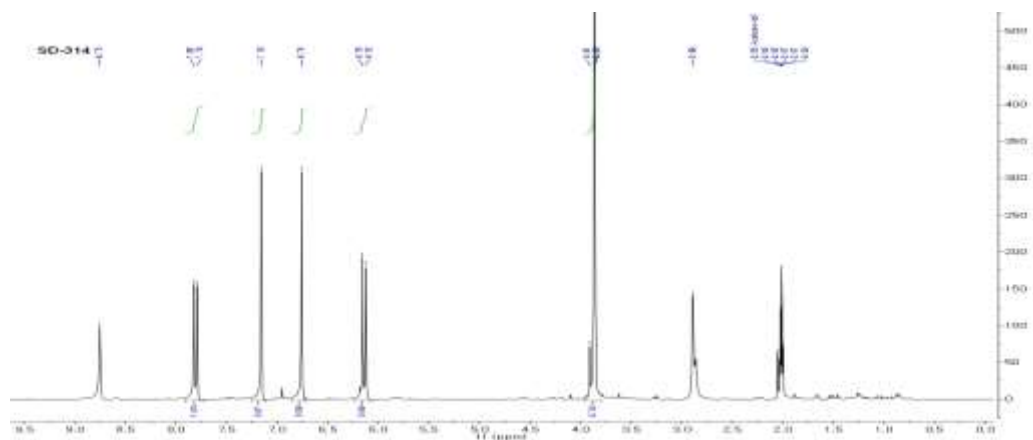


Figure 22.  $^1\text{H-NMR}$  spectrum of compound **7** (300 MHz, Acetone- $d_6$ )

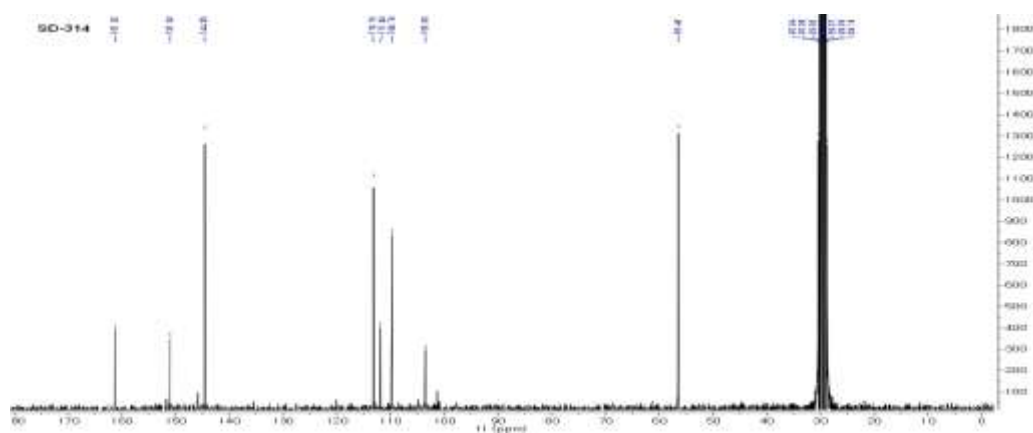


Figure 23.  $^{13}\text{C-NMR}$  spectrum of compound **7** (75 MHz, Acetone- $d_6$ )

### 1.2.8. Structure determination of compound **8**

Compound **8** was purified as light yellow needles with the molecular formula  $\text{C}_{16}\text{H}_{16}\text{O}_6$ . The  $^1\text{H-NMR}$  and  $^{13}\text{C-NMR}$  (Acetone- $d_6$ ) spectra of compound **8** showed the presence of a linear furanocoumarin nucleus substituted in position 5 and signals for two methyl group

attached to quaternary carbon atoms with hydroxyl group [ $\delta$  1.25 & 1.29 (s, 3H each)] and a Ar-O-CH<sub>2</sub>CH grouping [ $\delta$  4.44 & 4.86 (2H), 3.89 (1H)]. Thus, the structure of compound 8 was determined to be oxypeucedanin hydrate.<sup>69</sup>

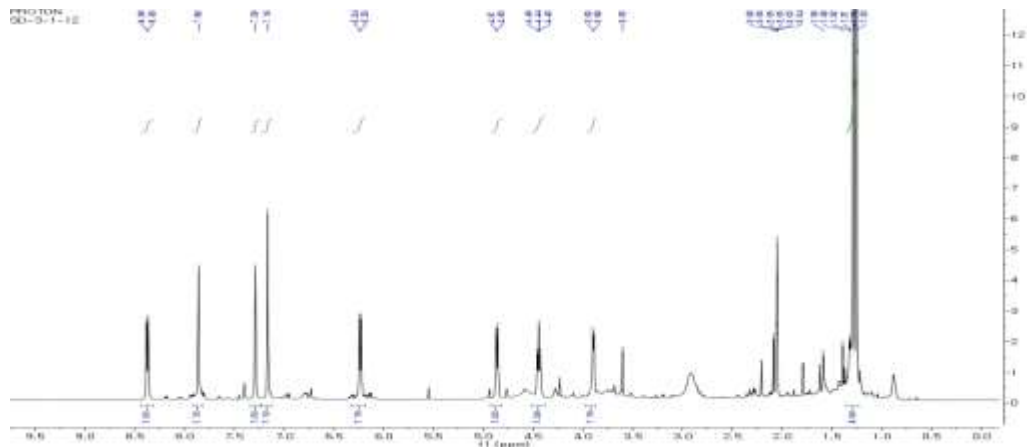


Figure 24. <sup>1</sup>H-NMR spectrum of compound 8 (500 MHz, Acetone-*d*<sub>6</sub>)

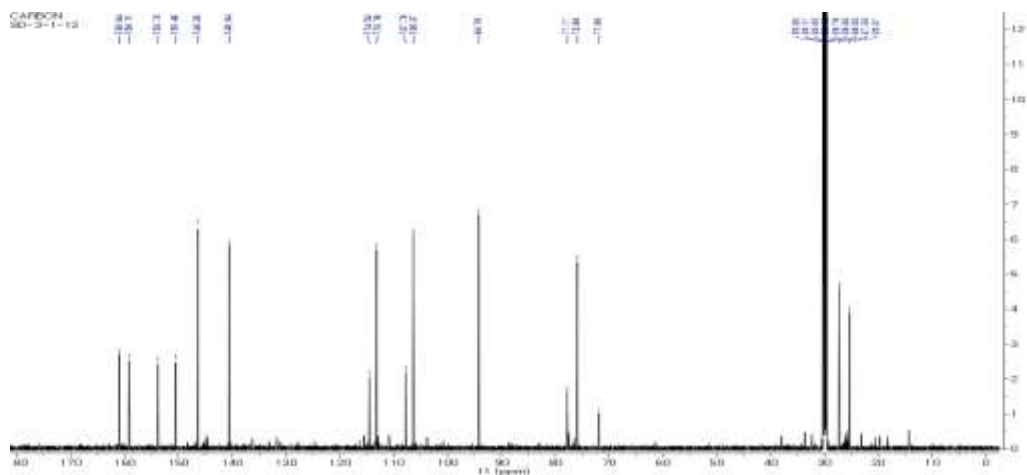


Figure 25. <sup>13</sup>C-NMR spectrum of compound 8 (125 MHz, Acetone-*d*<sub>6</sub>)

**Table 4 :**  $^1\text{H}$  and  $^{13}\text{C}$  NMR data for compounds **7** and **8**

Pos.	7		8	
	$\delta_{\text{H}}$ mult.(J in Hz)	$\delta_{\text{C}}$	$\delta_{\text{H}}$ mult.(J in Hz)	$\delta_{\text{C}}$
2		161.4		160.9
3	6.17 d (9.5)	110.0	6.23 d (9.7)	113.2
4	7.85 d (9.5)	144.7	8.37 d (9.7)	140.5
5	7.18 s	103.8		150.4
6		146.0		114.5
7		151.1		159.1
8	6.74 s	113.4	7.16 s	94.2
9		151.8		153.7
10		112.1		107.8
6-OCH <sub>3</sub>	3.94 s	56.7		
1'			7.29 d (2.5)	103.3
2'			7.86 d (2.5)	146
3'				
3'Gem				
1'''			4.44 t (9.0)	75.9
			4.86 d (9.0)	
2'''			3.89 d (9.0)	77.8
3'''				71.9
4'''			1.25 s	27.2
5'''			1.29 s	25.4

### 1.2.9. Structure determination of compound **9**

Compound **9** was purified as white powder with the molecular formula  $\text{C}_{14}\text{H}_{14}\text{O}_4$ . The  $^1\text{H}$ -NMR and  $^{13}\text{C}$ -NMR (Acetone- $d_6$ ) spectra of compound showed the presence of a linear pyranocoumarin nucleus [ $\delta$  6.13 (d,  $J=9.5$  Hz, 3-H), 7.87 (d,  $J=9.5$  Hz, 4-H), 7.42 (s, 5-H), 6.73 (s, 8-H), 1.24, 1.25 (both s, 2'-CH<sub>3</sub>), 3.67 (dd,  $J=10.5$ , 2.0 Hz, 3'-H), 3.07 (dd,  $J=14.0$ , 2.0 Hz, 4'-H), 2.53 (dd,  $J=14.0$ , 10.5 Hz, 4'-H)] with 3' position hydroxyl substitution. The structure of compound **9** was determined to be decurcinol.<sup>70</sup>

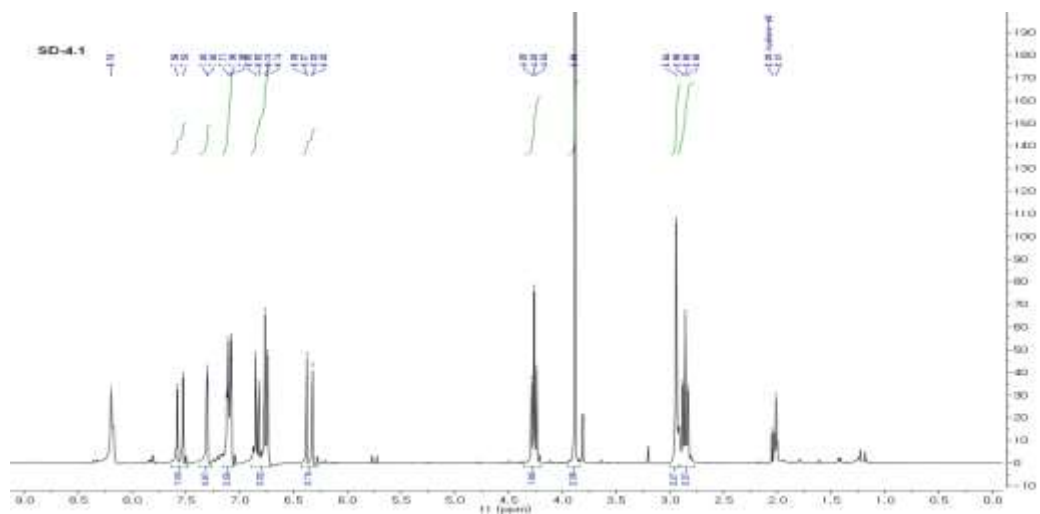


Figure 26.  $^1\text{H-NMR}$  spectrum of compound 9 (300 MHz, Acetone- $d_6$ )

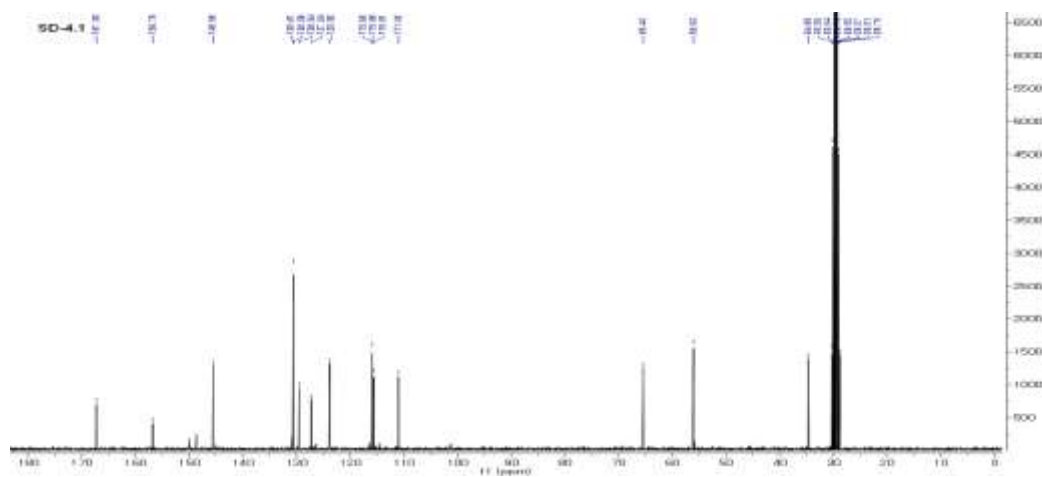


Figure 27.  $^{13}\text{C-NMR}$  spectrum of compound 9 (75 MHz, Acetone- $d_6$ )

### 1.2.10. Structure determination of compound 10

Compound **10** was purified as white powder with the molecular formula  $C_9H_6O_3$ . The  $^1H$ -NMR and  $^{13}C$ -NMR (Acetone- $d_6$ ) spectra of compound showed the presence of a coumarin skeleton [ $\delta$  6.17 (d,  $J=9.5$  Hz, 3-H), 7.85 (d,  $J=9.5$  Hz, 4-H), 6.74 (d,  $J=2.0$  Hz, 5-H), 6.85 (dd,  $J=8.4, 2.0$  Hz, 6-H), 7.50 (d,  $J=8.4$  Hz, 8-H)] with hydroxyl group substitution at 7-position. The structure of compound **10** was determined to be umbelliferone.<sup>71</sup>

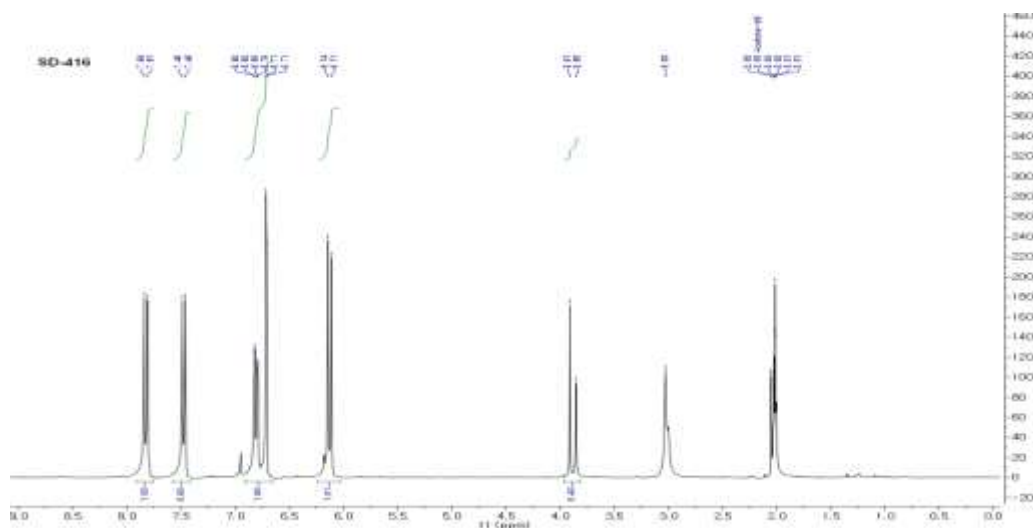


Figure 28.  $^1H$ -NMR spectrum of compound **10** (300 MHz, Acetone- $d_6$ )



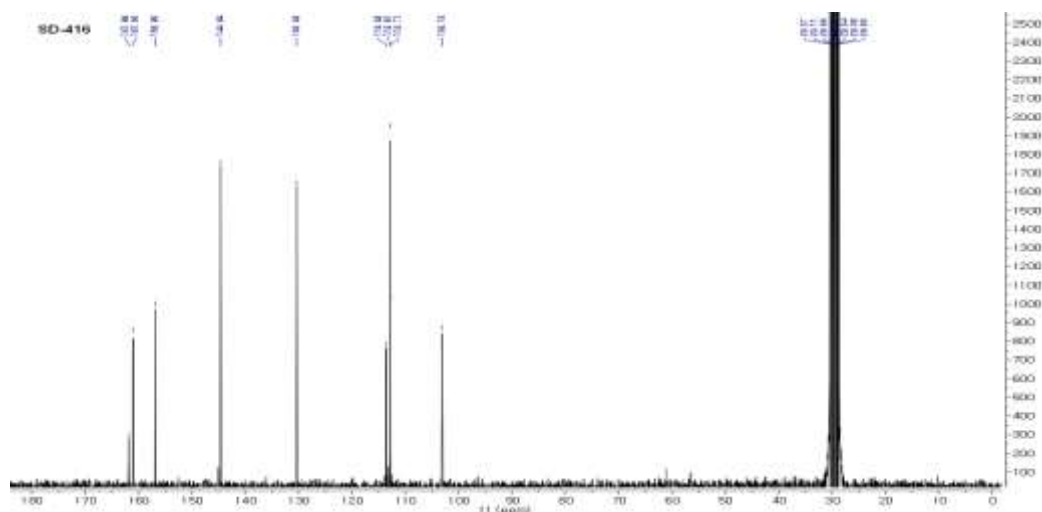


Figure 29.  $^{13}\text{C}$ -NMR spectrum of compound **10** (75 MHz, Acetone- $d_6$ )

Table 5 :  $^1\text{H}$  and  $^{13}\text{C}$  NMR data for compounds **9** and **10**.

Pos.	9		10	
	$\delta_{\text{H}}$ mult.(J in Hz)	$\delta_{\text{C}}$	$\delta_{\text{H}}$ mult.(J in Hz)	$\delta_{\text{C}}$
2		160.1		161.1
3	6.13 d (9.5)	113.1	6.17 d (9.5)	110.0
4	7.87 d (9.5)	145.0	7.85 d (9.5)	144.7
5	7.42 s	131.6	6.74 d (2.0)	103.8
6		113.0	6.85 dd (8.4, 2.0)	130.5
7		161.0		162.0
8	6.73 s	103.9	7.50 d (8.4)	113.4
9		155.8		157.0
10		126.0		112.1
6-OCH <sub>3</sub>				
1'	3.07 dd (14.0, 2.0)	33.9		
	2.53 dd (14.0, 10.5)			
2'	3.67 dd (10.5, 2.0)		73.0	
3'		80.3		
3'Gem	1.25 s	25.6		
	1.24 s	25.5		

## 1.4. Anti-viral activity of isolated compounds against PED virus

### 1.2.1. Determination of TCID<sub>50</sub> of stock PED virus suspension

Estimation of the lethality of virus is essential to ensure the uniform viral challenge throughout the experiments, for which various methods are used to indicate the active viral concentration in a suspension like plaque forming unit per mL (PFU/mL), multiplicity of Infection (MOI), 50% tissue culture infectious dose (TCID<sub>50</sub>) etc. This study being cell culture based, TCID<sub>50</sub> was chosen for measuring the strength of stock viral suspension.

TCID<sub>50</sub> (50 % Tissue culture infectious dose) is concentration of virus which induces cytopathic effect in 50 % of the cells in a tissue culture. The TCID<sub>50</sub> was determined to be 880.4 x dilution of the stock virus suspension. Thus, in the experiments 200 x dilution was used which is (880.4/200=) 4.4TCID<sub>50</sub>.

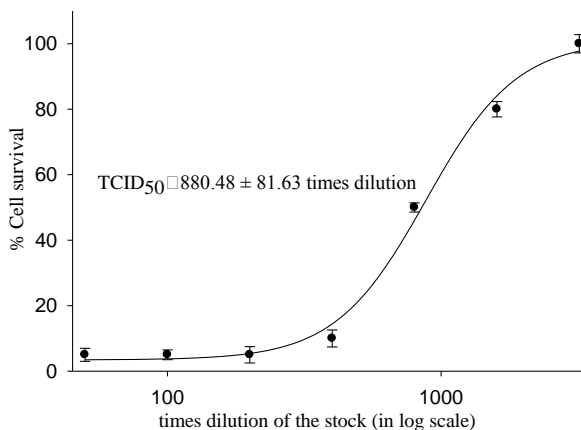


**Figure 30. PED virus titration curve for TCID<sub>50</sub> determination.**

880.48 times dilution of the virus stock was found to inhibit 50 % of the cultured vero cells.

### 1.2.2. Assessment of PEDV induced CPE inhibitory activities of isolated compounds:

Bioactivity guided successive fractionation of radix *S. divaricata* led to isolation of 6 angular pyrano coumarins (Khellactones) (**1** to **6**), two simple coumarins derivatives (**7** and **10**), a furano coumarin derivative and a linear pyrano coumarin (**9**). All isolates were tested for inhibitory activity against PEDV induced CPE. Angular pyrano-coumarin (Khellactone) (fig. 43A) derivatives have previously been found to have antiviral activity.<sup>57-59</sup> Indeed, among the isolates, those with khellactone moiety (**1** to **6**) were found to inhibit PEDV induced CPE in vero cells, in contrast **7** – **10**, which don't have that skeleton, did not show any significant CPE inhibition. Although 3'C substituted khellactones are also reported to be cytotoxic,<sup>72, 73</sup> observations in this study shows that, in addition to toxicity such substitution also leads to increased potency. As we can see, **2** and **6**, with small or no substitution in 3'C position, showed good activity with low toxicity, while **1**, **3-5**, which have bulky substitutions at 3'C had higher antiviral potency as well as toxicity. (Table 2)

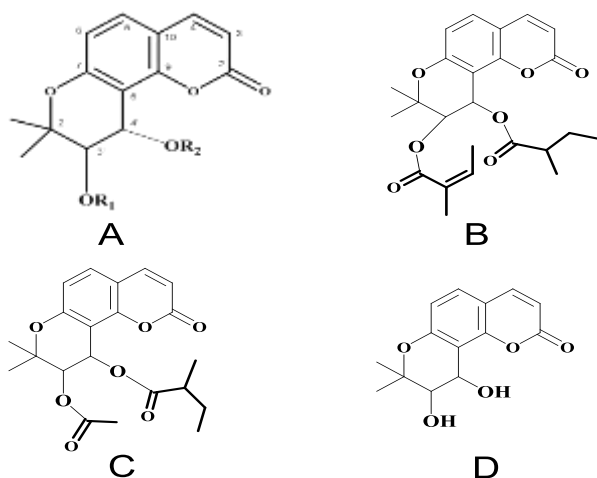


**Figure 31. A. Khellactone (angular pyrano coumarin) skeleton; B. Compound 1; C. Compound 2; D. Compound 6**

**Table 6. Inhibitory effects of compounds 1 – 10 on PEDV induced CPE**

Compound	Activity EC <sub>50</sub> ( $\mu$ M) <sup>a</sup>	Cytotoxicity CC <sub>50</sub> ( $\mu$ M) <sup>a</sup>	Safety Index
<b>2</b>	5.91	> 50	>8.4
<b>6</b>	15.26	> 50	>3.27
Ribavirin <sup>b</sup>	13.98	> 50	>3.57

Compound	Optimum Concentration( $\mu$ M) <sup>a</sup>	% CPE Inhibition <sup>a</sup>	Cytotoxicity CC <sub>50</sub> ( $\mu$ M) <sup>a</sup>
<b>1</b>	6.12	68.7	1.67 $\pm$ 0.16
<b>3</b>	3.07	40.5	1.93 $\pm$ 0.22
<b>4</b>	6.15	49.0	1.93 $\pm$ 0.45
<b>5</b>	0.73	32.5	0.54 $\pm$ 0.08
<b>7</b>	NA <sup>c</sup>	-	NT <sup>d</sup>
<b>8</b>	NA <sup>c</sup>	-	NT <sup>d</sup>
<b>9</b>	NA <sup>c</sup>	-	NT <sup>d</sup>
<b>10</b>	NA <sup>c</sup>	-	NT <sup>d</sup>

EC<sub>50</sub> : 50 % Effective concentration; CC<sub>50</sub> : 50 % Cytotoxic concentration; SI : Safety Index

<sup>a</sup> Tests were carried out in triplicate

<sup>b</sup> The compound was used as the positive control

<sup>c</sup> No significant activity

<sup>d</sup> Not tested

Compound **2** and **6** showed excellent CPE inhibitory activity with safety indices more than 8 and 3.2 respectively. While **2** has an acetyl substitution at 3'C which leads to its higher potency inhibiting almost 98 % CPE at the concentration of 27.1  $\mu$ M but **6** doesn't have 3'substitution and thus inhibits about 93 % CPE at the concentration of 76.2  $\mu$ M, almost three times higher than that of **2**. The regression analysis showed the EC<sub>50</sub> of **2** and **6** to be 5.91  $\pm$  0.38  $\mu$ M and 15.26  $\pm$  0.82  $\mu$ M respectively, which is comparable to the positive control

Ribavirin ( $EC_{50} 13.98 \pm 1.71 \mu\text{M}$ ). Also the toxicity of these two compounds were very little even at high concentrations of  $50 \mu\text{M}$  of the former and  $76 \mu\text{M}$  of latter. Compound **2** didn't show any toxicity up to the concentration of  $27.14 \mu\text{M}$  but when the concentration was doubled to  $54.28 \mu\text{M}$ , slight toxicity was shown, with cell survival dropping to  $76.78 \%$ , while **6** didn't have noticeable toxicity upto  $76 \mu\text{M}$ . (Fig. 41) This difference in toxicity can also be related to the presence (**2**) or absence (**6**) of substituent at 3'C position.

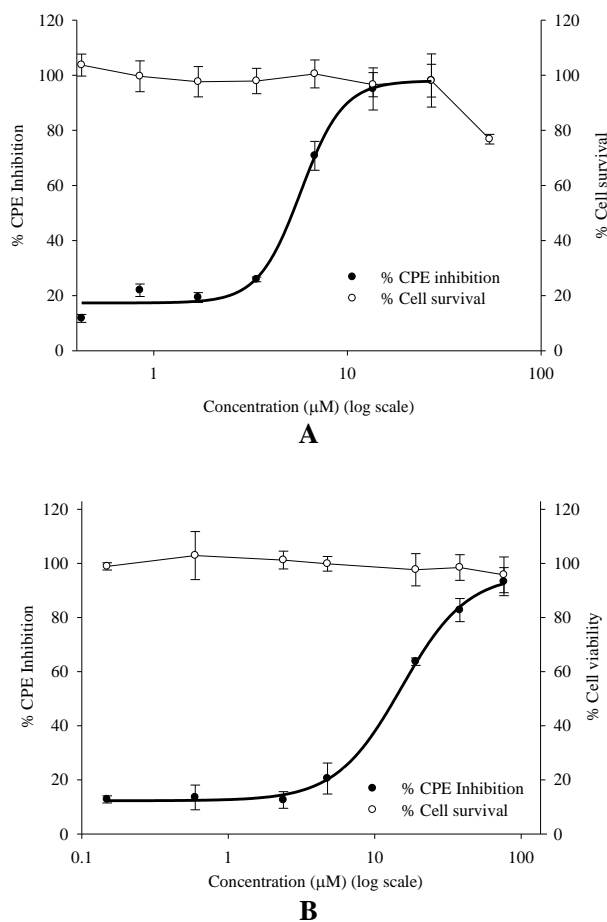


**Figure 32.** CPE inhibitory activity (black dots) and cell survival data (white dots) of compound **2** (A) and **6** (B).  $EC_{50}$  of **2** and **6** is  $5.91$  and  $15.26 \mu\text{M}$  respectively.

Due to the cytotoxicity, it was not possible to determine the EC<sub>50</sub> of compounds with bulky 3'C substituents (**1**, **3-5**), however at their optimum safe concentration they were highly potent. Compound **1** and **4** inhibited a maximum CPE of about 70 % and 40 % respectively at the concentration of 6.12 μM on the other hand compounds **3** and **5** inhibited 40.5 % and 34.3 % CPE at the concentration as small as 3.07 and 1.45 μM respectively.(Fig. 43) Above these concentrations all four compounds were found to exert cytotoxicity.

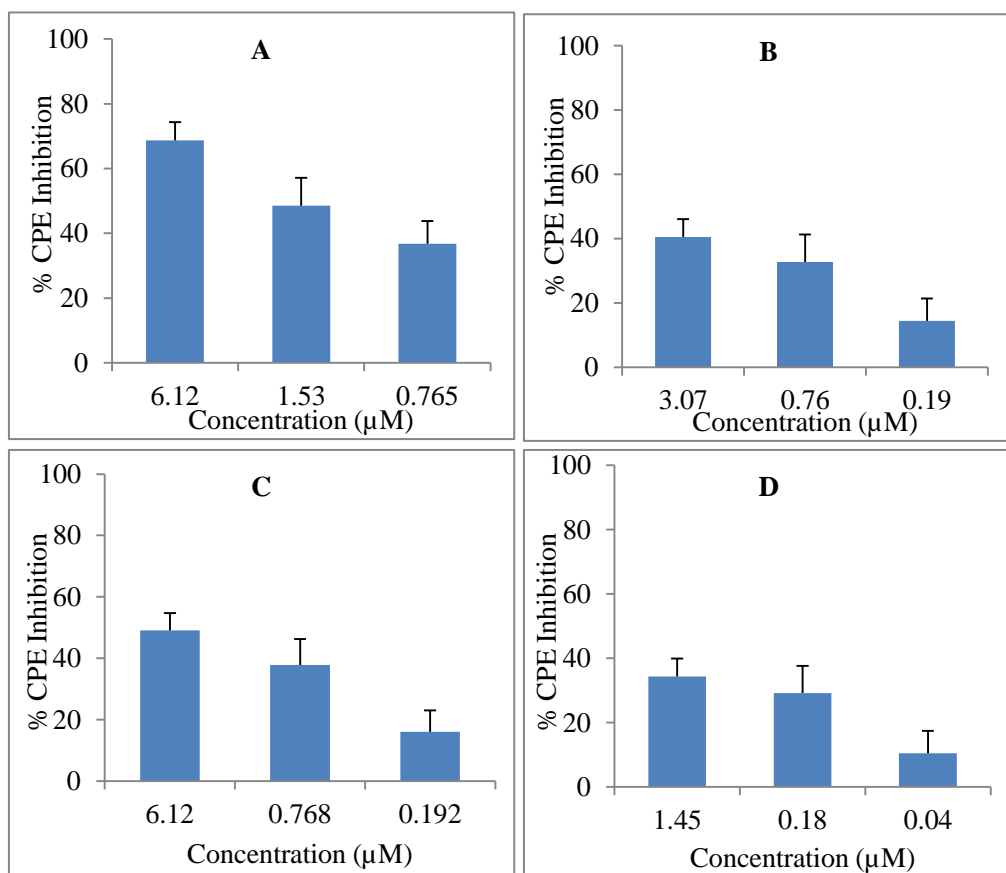


**Figure 33. Dose dependent activity of Compound 1 (A), 3 (B), 4 (C), 5 (D) against PEDV induced CPE in vero cells**

Comparison of the morphology of PEDV infected cells after treatment with khellactones with small and bulky 3'C substituent also showed convincing results. Two representative compounds, **1** having bulky and **6** with small substituent were chosen for study. The CPE inhibition in infected cells treated with 6.12  $\mu\text{M}$  or 3.6  $\mu\text{M}$  of compound **1** was significantly higher than the inhibition shown by **2** at 25.7  $\mu\text{M}$  and 12.8 $\mu\text{M}$ . The protection offered by **1** or **2** was comparable or even better than positive controls Ribavirin (41 $\mu\text{M}$ ) and glycyrrhizin (12 $\mu\text{M}$ ). (Fig. 45)

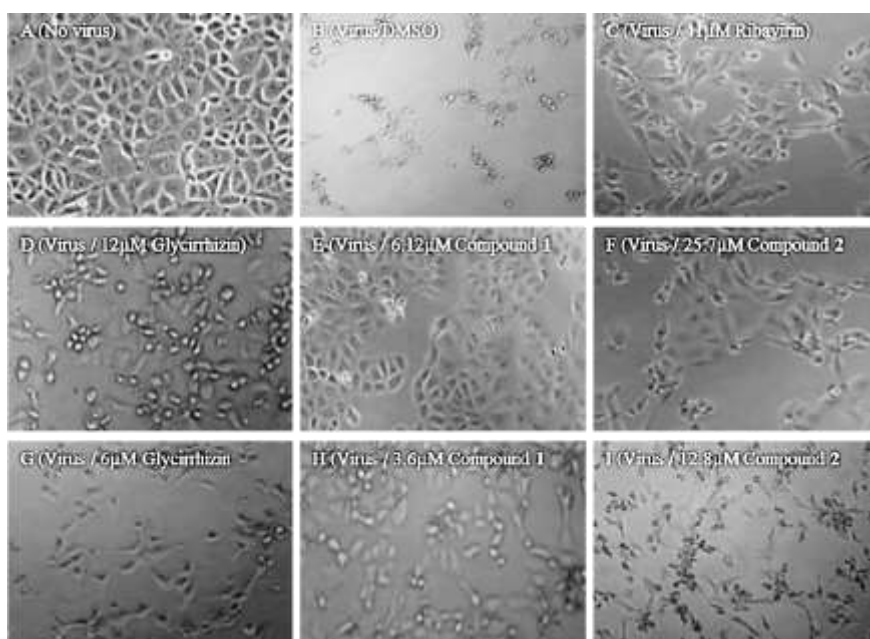


**Figure 34. Morphologies of Vero cells show the effects of compound 1, 2 and compounds used as positive controls, Ribavirin and Glycyrrhizin on PEDV-induced CPE. (A) Non-infected cells; (B) Mock (C) 41  $\mu\text{M}$  Ribavirin (D) 12  $\mu\text{M}$  of Glycyrrhizin (E) 6.12  $\mu\text{M}$  Compound 1 (F) 25.7  $\mu\text{M}$  Compound 2 (G) 6  $\mu\text{M}$  Glycyrrhizin (H) 3.6  $\mu\text{M}$  Compound 1 (I) 12.8  $\mu\text{M}$  Compound 2 treated PEDV-infected vero cells on fourth day of infection.**

## 4. Conclusions

PED is a serious illness in pigs with disastrous consequences in swine based agro-economy. No drugs are being effectively used to treat this ailment hitherto. Some vaccines however have been licensed in few countries, but their efficiency being not dependable, the swine industry is still in grave threat. Further, viruses, like SARS, from coronaviridae family have been culprit to human epidemics and still pose a threat with recently new Coronavirus being found killing few people in Arab regions. Being the members of same family of viruses they share some similar replication mechanism, hence the molecules against PED virus could be of significance for protection of humans too from the other Coronaviruses. Thus, with an objective of finding a safe and efficient compound against this virus, the plant *Saposhnikovia divaricata*, a popular ingredient of traditional Chinese medicine, was studied by bioactivity guided fractionation leading to isolation of 10 coumarin, among which six compounds inhibited the PED virus induced CPE.

Among the isolates, two compounds were found to have good antiviral property with little toxicity, hence leading to high safety index. The other four compounds were also able to inhibit the virus noticeably; however at higher concentrations they were found to exert cytotoxicity. The remaining four compounds, on the contrary didn't show significant antiviral activity. Further, this study also shows that angular pyrano coumarin structure or khellactone, have inhibitory activity against PED virus, and the substitution at the carbon 3' position leads to increase in anti-viral activity as well as cytotoxicity.

Thus, these compounds could be developed into new class of safe and efficient drugs against PED virus. Further studies on the mechanism of action would help to make these molecules more efficient drug against not only against PEDV but other Coronaviruses too.



## 5. References

1. Zimmerman, J.; Karriker, L.; Ramirez, A.; Schwartz, K.; Stevenson, G. *Diseases of Swine* Wiley: 2012.
2. Pospischil, A.; Stuedli, A.; Kiupel, M. Update on porcine epidemic diarrhea *J. Swine Health Prod.* **2002**, 10, (2), 81-85.
3. Pensaert, M. B.; de Bouck, P. A new coronavirus-like particle associated with diarrhea in swine *Arch. Virol.* **1978**, 58, (3), 243-7.
4. Pensaert, P. M. Porcine epidemic diarrhoea now enzootic in Asia (Special 2005). *Pig Progress* 2005.
5. Chae, C.; Kim, O.; Choi, C.; Min, K.; Cho, W.-S.; Kim, J.; Tai, J. H. Prevalence of porcine epidemic diarrhoea virus and transmissible gastroenteritis virus infection in Korean pigs *Vet. Rec.* **2000**, 147, (21), 606-608.
6. Martelli, P.; Lavazza, A.; Nigrelli, A. D.; Merialdi, G.; Alborali, L. G.; Pensaert, M. B. Epidemic of diarrhoea caused by porcine epidemic diarrhoea virus in Italy *Vet. Rec.* **2008**, 162, (10), 307-310.
7. Puranaveja, S.; Poolperm, P.; Lertwatcharasarakul, P.; Kesdaengsakonwut, S.; Boonsoongnern, A.; Urairong, K.; Kitikoon, P.; Choojai, P.; Kedkovid, R.; Teankum, K.; Thanawongnuwech, R. Chinese-like strain of porcine epidemic diarrhea virus, Thailand *Emerg. Infect. Dis.* **2009**, 15, (7), 1112-5.
8. Sun, R. Q.; Cai, R. J.; Chen, Y. Q.; Liang, P. S.; Chen, D. K.; Song, C. X. *Outbreak of porcine epidemic diarrhea in suckling piglets, China* *Emerg. Infect. Dis.* 2012 Jan;18(1):161-3. doi: 10.3201/eid1801.111259.

9. de Bouck, P.; Pensaert, M. B.; Coussement, W. The pathogenesis of an enteric infection in pigs, experimentally induced by the coronavirus-like agent, CV 777 *Vet. Microbiol.* **1981**, 6, (2), 157-165.
10. Pensaert, M. B. *Porcine Epidemic diarrhea virus* Iowa State University Press: Ames, Iowa, USA, 1999.
11. Chen, F.; Pan, Y.; Zhang, X.; Tian, X.; Wang, D.; Zhou, Q.; Song, Y.; Bi, Y. Complete genome sequence of a variant porcine epidemic diarrhea virus strain isolated in China *J. Virol.* **2012**, 86, (22), 12448.
12. Beaudette, F.; Hudson, C. Cultivation of the virus of infectious bronchitis *J. Am. Vet. Med. Assoc.* **1937**, 90, 51-60.
13. Cheever, F. S.; Daniels, J. B. A murine virus (JHM) causing disseminated encephalomyelitis with extensive destruction of myelin *J. Exp. Med.* **1949**, 90, (3), 181-210.
14. Doyle, L.; Hutchings, L. A transmissible gastroenteritis in pigs *J. Am. Vet. Med. Assoc.* **1946**, 108, 257-259.
15. Siddell, S.; Wege, H.; Ter Meulen, V. The Biology of Coronaviruses *J. Gen. Virol.* **1983**, 64, (4), 761-776.
16. Woo, P. C.; Lau, S. K.; Huang, Y.; Yuen, K. Y. Coronavirus diversity, phylogeny and interspecies jumping *Exp. Biol. Med.* **2009**, 234, (10), 1117-27.
17. Woo, P. C. Y.; Lau, S. K. P.; Li, K. S. M.; Poon, R. W. S.; Wong, B. H. L.; Tsoi, H.-w.; Yip, B. C. K.; Huang, Y.; Chan, K.-h.; Yuen, K.-y. Molecular diversity of coronaviruses in bats *Virology* **2006**, 351, (1), 180-187.
18. Woo, P. C.; Wang, M.; Lau, S. K.; Xu, H.; Poon, R. W.; Guo, R.; Wong, B. H.; Gao, K.; Tsoi, H. W.; Huang, Y.; Li, K. S.; Lam, C. S.; Chan, K. H.; Zheng, B. J.; Yuen, K.

- Y. Comparative analysis of twelve genomes of three novel group 2c and group 2d coronaviruses reveals unique group and subgroup features *J. Virol.* **2007**, 81, (4), 1574-85.
19. Duffy, S.; Shackelton, L. A.; Holmes, E. C. Rates of evolutionary change in viruses: patterns and determinants *Nat. Rev. Genet.* **2008**, 9, (4), 267-76.
20. Lai, M. M. RNA recombination in animal and plant viruses *Microbiol. Rev.* **1992**, 56, (1), 61-79.
21. Lau, S. K. P.; Woo, P. C. Y.; Li, K. S. M.; Huang, Y.; Tsoi, H.-W.; Wong, B. H. L.; Wong, S. S. Y.; Leung, S.-Y.; Chan, K.-H.; Yuen, K.-Y. Severe acute respiratory syndrome coronavirus-like virus in Chinese horseshoe bats *Proc. Natl. Acad. Sci. U.S.A* **2005**, 102, (39), 14040-14045.
22. David, R. New coronavirus *Nat. Rev. Microbiol.* **2012**, 10, (11), 730-730.
23. Zaki, A. M.; van Boheemen, S.; Bestebroer, T. M.; Osterhaus, A. D.; Fouchier, R. A. Isolation of a novel coronavirus from a man with pneumonia in Saudi Arabia *New. Engl. J. Med.* **2012**, 367, (19), 1814-1820.
24. Butler, D. Clusters of coronavirus cases put scientists on alert *Nature* **2012**.
25. Pritchard, C.; Paton, D.; Wibberley, G.; Iбата, G. Transmissible gastroenteritis and porcine epidemic diarrhoea in Britain *Vet. Rec.* **1999**, 144, (22), 616-618.
26. Park, S. J.; Song, D. S.; Park, B. K. Molecular epidemiology and phylogenetic analysis of porcine epidemic diarrhea virus (PEDV) field isolates in Korea *Arch. Virol.* **2013**, 6, 6.
27. Yeo, S. G.; Hernandez, M.; Krell, P. J.; Nagy, E. E. Cloning and sequence analysis of the spike gene of porcine epidemic diarrhea virus Chinju99 *Virus Genes* **2003**, 26, (3), 239-46.

28. Kweon, C. H.; Kwon, B. J.; Lee, J. G.; Kwon, G. O.; Kang, Y. B. Derivation of attenuated porcine epidemic diarrhea virus (PEDV) as vaccine candidate *Vaccine* **1999**, 17, (20-21), 2546-53.
29. Song, D. S.; Oh, J. S.; Kang, B. K.; Yang, J. S.; Moon, H. J.; Yoo, H. S.; Jang, Y. S.; Park, B. K. Oral efficacy of Vero cell attenuated porcine epidemic diarrhea virus DR13 strain *Res. Vet. Sci.* **2007**, 82, (1), 134-140.
30. Suo, S.; Ren, Y.; Li, G.; Zarlenga, D.; Bu, R.-e.; Su, D.; Li, X.; Li, P.; Meng, F.; Wang, C.; Ren, X. Immune responses induced by DNA vaccines bearing Spike gene of PEDV combined with porcine IL-18 *Virus Res.* **2012**, 167, (2), 259-266.
31. Duarte, M.; Laude, H. Sequence of the spike protein of the porcine epidemic diarrhoea virus *J. Gen. Virol.* **1994**, 75, (Pt 5), 1195-200.
32. Chang, S. H.; Bae, J. L.; Kang, T. J.; Kim, J.; Chung, G. H.; Lim, C. W.; Laude, H.; Yang, M. S.; Jang, Y. S. Identification of the epitope region capable of inducing neutralizing antibodies against the porcine epidemic diarrhea virus *Mol. Cells* **2002**, 14, (2), 295-299.
33. Cruz, D. J. M.; Kim, C.-J.; Shin, H.-J. The GPRLQPY motif located at the carboxy-terminal of the spike protein induces antibodies that neutralize Porcine epidemic diarrhea virus *Virus. Res.* **2008**, 132, (1-2), 192-196.
34. Bosch, B. J.; van der Zee, R.; de Haan, C. A.; Rottier, P. J. The coronavirus spike protein is a class I virus fusion protein: structural and functional characterization of the fusion core complex *J. Virol.* **2003**, 77, (16), 8801-11.
35. Song, D.; Park, B. Porcine epidemic diarrhoea virus: a comprehensive review of molecular epidemiology, diagnosis, and vaccines *Virus Genes* **2012**, 44, (2), 167-75.

36. Wu, J.-N. *Chinese Materia Medica*. Oxford University Press, Inc.: 198 Madison Avenue, New York, 2005.
37. Xue, B. Y.; Li, W.; Li, L.; Xiao, Y. Q. [A pharmacodynamic research on chromone glucosides of fangfeng] *Zhongguo Zhong Yao Za Zhi* **2000**, 25, (5), 297-9.
38. Yang, L.-L.; Lo, Y.; Chen, L. Cimifugin preparation and quantitative analysis of *Saposhnikovia Radix* by HPLC *J. Food. Drug. Anal.* **1999**, 7, (3), 191-197.
39. Jiang, Y. Y.; Liu, B.; Shi, R. B.; Tu, G. Z. [Isolation and structure identification of chemical constituents from *Saposhnikovia divaricata* (Turcz.) Schischk] *Yao Xue Xue Bao* **2007**, 42, (5), 505-10.
40. Li, W.; Wang, Z.; Sun, Y. S.; Chen, L.; Han, L. K.; Zheng, Y. N. Application of response surface methodology to optimise ultrasonic-assisted extraction of four chromones in *Radix Saposhnikovia* *Phytochem. Anal.* **2011**, 22, (4), 313-21.
41. Li, L.; Liu, Y. Y.; Geng, L. D.; Xiao, Y. Q. [Determination of four components in root of *Saposhnikovia divaricata* by HPLC gradient elution] *Zhongguo Zhong Yao Za Zhi* **2006**, 31, (3), 194-6.
42. Okuyama, E.; Hasegawa, T.; Matsushita, T.; Fujimoto, H.; Ishibashi, M.; Yamazaki, M. Analgesic components of *saposhnikovia* root (*Saposhnikovia divaricata*) *Chem. Pharm. Bull.* **2001**, 49, (2), 154-60.
43. Tai, J.; Cheung, S. Anti-proliferative and antioxidant activities of *Saposhnikovia divaricata* *Oncol. Rep.* **2007**, 18, (1), 227-34.
44. Kim, T. H.; Yoon, S. J.; Lee, W. C.; Kim, J. K.; Shin, J.; Lee, S.; Lee, S. M. Protective effect of GCSB-5, an herbal preparation, against peripheral nerve injury in rats *J. Ethnopharmacol.* **2011**, 136, (2), 297-304.

45. Shimizu, N.; Tomoda, M.; Gonda, R.; Kanari, M.; Takanashi, N.; Takahashi, N. The major pectic arabinogalactan having activity on the reticuloendothelial system from the roots and rhizomes of *Saposhnikovia divaricata* *Chem. Pharm. Bull.* **1989**, 37, (5), 1329-32.
46. Hoult, J.; Paya, M. Pharmacological and biochemical actions of simple coumarins: natural products with therapeutic potential *Gen. Pharmacol.-Vasc. S.* **1996**, 27, (4), 713-722.
47. Piller, N. B. A comparison of the effectiveness of some anti-inflammatory drugs on thermal oedema *Br. J. Exp. Pathol.* **1975**, 56, (6), 554-60.
48. Huang, G. J.; Deng, J. S.; Liao, J. C.; Hou, W. C.; Wang, S. Y.; Sung, P. J.; Kuo, Y. H. Inducible nitric oxide synthase and cyclooxygenase-2 participate in anti-inflammatory activity of imperatorin from *Glehnia littoralis* *J. Agric. Food Chem.* **2012**, 60, (7), 1673-81.
49. Basile, A.; Sorbo, S.; Spadaro, V.; Bruno, M.; Maggio, A.; Faraone, N.; Rosselli, S. Antimicrobial and antioxidant activities of coumarins from the roots of *Ferulago campestris* (Apiaceae) *Molecules* **2009**, 14, (3), 939-52.
50. Raja, S. B.; Murali, M. R.; Roopa, K.; Devaraj, S. N. Imperatorin a furocoumarin inhibits periplasmic Cu-Zn SOD of *Shigella dysenteriae* their by modulates its resistance towards phagocytosis during host pathogen interaction *Biomed. Pharmacother.* **2011**, 65, (8), 560-8.
51. Wang, C. M.; Zhou, W.; Li, C. X.; Chen, H.; Shi, Z. Q.; Fan, Y. J. Efficacy of osthol, a potent coumarin compound, in controlling powdery mildew caused by *Sphaerotheca fuliginea* *J. Asian. Nat. Prod. Res.* **2009**, 11, (9), 783-91.

52. Zhang, L.; Jiang, G.; Yao, F.; He, Y.; Liang, G.; Zhang, Y.; Hu, B.; Wu, Y.; Li, Y.; Liu, H. Growth inhibition and apoptosis induced by osthole, a natural coumarin, in hepatocellular carcinoma *PLoS One* **2012**, 7, (5), 25.
53. Kawase, M.; Sakagami, H.; Motohashi, N.; Hauer, H.; Chatterjee, S. S.; Spengler, G.; Vigiyanne, A. V.; Molnar, A.; Molnar, J. Coumarin derivatives with tumor-specific cytotoxicity and multidrug resistance reversal activity *In Vivo* **2005**, 19, (4), 705-11.
54. MA, J. Y.; UM, Y. R.; LEE, J. H. Composition for preventing and treating influenza-virus-induced diseases. In WO Patent 2,011,055,881: 2011.
55. Ma, S.-C.; Du, J.; But, P. P.-H.; Deng, X.-L.; Zhang, Y.-W.; Ooi, V. E.-C.; Xu, H.-X.; Lee, S. H.-S.; Lee, S. F. Antiviral Chinese medicinal herbs against respiratory syncytial virus *J. Ethnopharmacol.* **2002**, 79, (2), 205-211.
56. Kato, T.; Horie, N.; Matsuta, T.; Naoki, U.; Shimoyama, T.; Kaneko, T.; Kanamoto, T.; Terakubo, S.; Nakashima, H.; Kusama, K.; Sakagami, H. Anti-UV/HIV activity of Kampo medicines and constituent plant extracts *In Vivo* **2012**, 26, (6), 1007-13.
57. Spino, C.; Dodier, M.; Sotheeswaran, S. Anti-HIV coumarins from *Calophyllum* seed oil *Bioorg. Med. Chem. Lett.* **1998**, 8, (24), 3475-8.
58. McKee, T. C.; Fuller, R. W.; Covington, C. D.; Cardellina, J. H., 2nd; Gulakowski, R. J.; Krepps, B. L.; McMahon, J. B.; Boyd, M. R. New pyranocoumarins isolated from *Calophyllum lanigerum* and *Calophyllum teysmannii* *J. Nat. Prod.* **1996**, 59, (8), 754-8.
59. Tang, J.; Qian, K.; Zhang, B. N.; Chen, Y.; Xia, P.; Yu, D.; Xia, Y.; Yang, Z. Y.; Chen, C. H.; Morris-Natschke, S. L.; Lee, K. H. Anti-AIDS agents 82: synthesis of seco-(3'R,4'R)-3',4'-di-O-(S)-camphanoyl-(+)-cis-khellactone (DCK) derivatives as novel anti-HIV agents *Bioorg. Med. Chem.* **2010**, 18, (12), 4363-73.

60. Wagner, E. K.; Hewlett, M. J.; Bloom, D. C.; Camerini, D. *Basic virology* Wiley-Blackwell: 2009.
61. McAleer, W. J.; Miller, W. J.; Hurni, W. M.; Machlowitz, R. A.; Hilleman, M. R. Automated cytopathic effect (CPE) assays *J. Biol. Stand.* **1983**, 11, (3), 241-6.
62. Heldt, C. L.; Hernandez, R.; Mudiganti, U.; Gurgel, P. V.; Brown, D. T.; Carbonell, R. G. A colorimetric assay for viral agents that produce cytopathic effects *J. Virol. Methods* **2006**, 135, (1), 56-65.
63. Matsuda, H.; Murakami, T.; Nishida, N.; Kageura, T.; Yoshikawa, M. Medicinal foodstuffs. XX. Vasorelaxant active constituents from the roots of *Angelica furcijuga* Kitagawa: structures of hyuganins A, B, C, and D *Chem. Pharm. Bull.* **2000**, 48, (10), 1429-35.
64. Liu, R.; Feng, L.; Sun, A.; Kong, L. Preparative isolation and purification of coumarins from *Peucedanum praeruptorum* Dunn by high-speed counter-current chromatography *J. Chromatogr. A* **2004**, 19, 1-2.
65. Jong, T. T.; Hwang, H. C.; Jean, M. Y.; Wu, T. S.; Teng, C. M. An antiplatelet aggregation principle and X-ray structural analysis of cis-khellactone diester from *Peucedanum japonicum* *J. Nat. Prod.* **1992**, 55, (10), 1396-401.
66. Chen, I.-S.; Chang, C.-T.; Sheen, W.-S.; Teng, C.-M.; Tsai, I.-L.; Duh, C.-Y.; Ko, F.-N. Coumarins and antiplatelet aggregation constituents from formosan *Peucedanum japonicum* *Phytochemistry* **1996**, 41, (2), 525-530.
67. Macías, F. A.; Massanet, G. M.; Rodríguez-Luis, F.; Salvá, J.; Fronczek, F. R. 13C NMR of coumarins. II—Khellactones: Spectroscopic criteria to establish the relative configuration of the dihydropyran ring *Magn. Reson. Chem.* **1989**, 27, (7), 653-658.



68. Adfa, M.; Yoshimura, T.; Komura, K.; Koketsu, M. Antitermite activities of coumarin derivatives and scopoletin from *Protium javanicum* Burm. f *J. Chem. Ecol.* **2010**, 36, (7), 720-6.
69. Fujioka, T.; Furumi, K.; Fujii, H.; Okabe, H.; Mihashi, K.; Nakano, Y.; Matsunaga, H.; Katano, M.; Mori, M. Antiproliferative constituents from umbelliferae plants. V. A new furanocoumarin and faltarindiol furanocoumarin ethers from the root of *Angelica japonica* *Chem. Pharm. Bull.* **1999**, 47, (1), 96-100.
70. Kim, S.; Ko, H.; Son, S.; Shin, K. J.; Kim, D. J. Enantioselective syntheses of (+)-decursinol and (+)-trans-decursidinol *Tetrahedron Lett.* **2001**, 42, (43), 7641-7643.
71. Singh, R.; Singh, B.; Singh, S.; Kumar, N.; Kumar, S.; Arora, S. Umbelliferone – An antioxidant isolated from *Acacia nilotica* (L.) Willd. Ex. Del *Food. Chem.* **2010**, 120, (3), 825-830.
72. Takeuchi, Y.; Xie, L.; Cosentino, L. M.; Lee, K.-H. Anti-AIDS agents-XXVIII.1 Synthesis and Anti-HIV activity of methoxy substituted 3',4'-Di-O(-)-camphanoyl-(+)-cis-khellactone (DCK) analogues *Bioorg. Med. Chem. Lett.* **1997**, 7, (20), 2573-2578.
73. Chang-yih, D.; Shang-Kwei, W.; Yang-Chang, W. Cytotoxic pyranocoumarins from the aerial parts of *Peucedanum japonicum* *Phytochemistry* **1991**, 30, (8), 2812-2814.

## 6. Acknowledgements

In my culture there is a belief we follow, “Dhyana moolam guru’r murti, Pooja moolam guru padam, Mantra moolam guru vakyam, Mokshya moolam guru kripa”. This means, “The source for my thinking is the image of my teacher (Guru), basis of my worship is his feet, my mantra is his words and his grace is my salvation.” Indeed, my professors ‘Guru’ have given me these feelings. I offer my perpetual respect with a bowed head and closed eyes to my advisor, Prof. Choi Hong Seok and Co-Advisor Prof. Oh Won Keun who deemed me suitable for including in their research team. Their encouragement, enthusiasm, supervision and perpetual demand for excellence, both scientifically and professionally, have transformed my thinking and given me a foresight to the future.

During the completion of my course, I wouldn’t have been able to succeed without the impressive and bound less helps of my lab members Dang Thai Trung, Kim JaYeon, Dao Trong Tuan, Tran Tien Lam, Dhodary Basanta and rest of the lab members. I am thankful to them for their excellent assistance and significant contribution.

I would also like to express my sincere gratitude to all professors and colleagues at College of Pharmacy, Chosun University as well as Seoul National University for their invaluable mentoring, support and emotional encouragement during my graduate training.

Finally, my work would not have been possible without the unfailing support of my family and my friends. I would like to express my special thanks to them for their patience, constant encouragement, and enthusiasm which have sustained my endeavor to complete my work.

*Korea, May 2013*

**Sharma Govinda**